Journal of Medicinal Chemistry

Article

A Sydnone Cycloaddition Route to Pyrazole-Based Analogs of Combretastatin A4

Andrew W. Brown, Matthew Fisher, Gillian M. Tozer, Chryso Kanthou, and Joseph P.A. Harrity

J. Med. Chem., **Just Accepted Manuscript** • DOI: 10.1021/acs.jmedchem.6b01128 • Publication Date (Web): 02 Oct 2016

Just Accepted

ACS Publications

Journal of Medicinal Chemistry is published by the American Chemical Society. 1155 Sixteenth Street N.W., Washington, DC 20036

A Sydnone Cycloaddition Route to Pyrazole-Based Analogs of Combretastatin A4

Andrew W. Brown,[†,‡] Matthew Fisher,[‡] Gillian M. Tozer,*[,‡] Chryso Kanthou,*[,‡] Joseph P. A. Harrity*[,†]

[†] Department of Chemistry, Dainton Building, Brook Hill, University of Sheffield, S3 7HF

[‡] Department of Oncology & Metabolism, The Medical School, University of Sheffield, Beech Hill Road, S10 2RX

Abstract

The combretastatins are an important class of tubulin-binding agents. Of this family, a number of compounds are potent tumor Vascular Disrupting Agents (VDAs) and have shown promise in the clinic for cancer therapy. We have developed a modular synthetic route to combretastatin analogs based on a pyrazole core through highly-regioselective alkyne cycloaddition reactions of sydnones. These compounds show modest to high potency against human umbilical vein endothelial cell proliferation. Moreover, evidence is presented that these novel VDAs have the same mode of action as CA4P and bind reversibly to β-tubulin – believed to be a key feature in avoiding toxicity. The most active compound from *in vitro* studies was taken forward to an *in vivo* model and instigated an increase in tumor cell necrosis.

Introduction

Tumor growth and metastasis are dependent upon a functional blood vessel network[1] and, since tumor blood vessels are abnormal, they represent an attractive target for cancer therapy.[2,3] Tumor Vascular Disrupting Agents (VDAs) cause a rapid and selective collapse of tumor blood vessels leading to widespread tumor cell death *via* necrosis.[4] The most well-studied class of VDAs are the tubulin binding microtubule depolymerizing agents. The tumor

vascular disrupting properties of colchicine, the classic tubulin binding agent of this type, have been known since the 1930s, but these effects are only seen at near to the maximum tolerated dose (MTD) in mice.[5,6] The structurally related stilbene compounds, the combretastatins, were isolated from the Cape Bush Willow tree, *Combretum caffrum* in the late 1980s.[7] These compounds were initially studied for their potential as antimitotic agents.[8] However, it later became apparent that the combretastatins had great potential as VDAs.[9] The lead compound, combretastatin A-4 (CA4), was shown to be effective at causing selective tumor vascular collapse, within minutes, at non-toxic doses.[10] It was swiftly developed into the water-soluble, sodium phosphate salt prodrug, disodium combretastatin A-4 3-*O*-phosphate (CA4P).[11] CA4P is not active as a tubulin binding agent, but is rapidly cleaved in plasma to CA4.[12] The lower toxicity (and thus higher MTD) of CA4 compared to colchicine is attributed to CA4 binding reversibly to the β-tubulin subunit, as opposed to colchicine that binds pseudo-irreversibly.[13] CA4P is currently undergoing Phase II/III clinical trials in combination with bevacizumab.[14]

Although CA4P is a promising clinical candidate, it does have a number of issues associated with it. Firstly, the *cis* orientation of the olefinic linker is key to activity, with the *trans* isomer being essentially inactive[15] – an issue further emphasized by the tendency of *cis* stilbenes to undergo *cis*-*trans* isomerization in heat, light and protic media.[16] A promising strategy to overcome this issue has been the incorporation of heterocyclic motifs to replace the olefinic linker.[17,18,19,20,21,22,23] This strategy allows the *cis* configuration of the combretastatins to be "fixed", inhibiting metabolic decomposition (*Figure 1*). However, any compound design would have to take into account the result of molecular docking studies that clearly indicate the need for appropriately disposed electron rich aryl rings, such as those in colchicine and CA4, which are key pharmacophores for tubulin polymerization inhibition.[24,25,26]

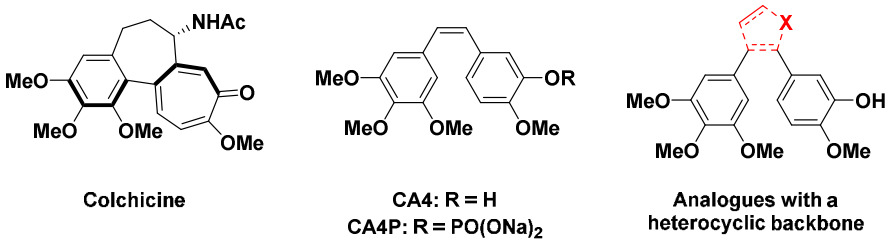

Figure 1. Tubulin-binding VDAs

Although a number of significant contributions have been made in the field of rigid combretastatin analogs, only limited examples of this approach using a pyrazole core have been documented.[16,20,27,28] To the best of our knowledge, there are no examples of simple (without extra substitution of the pyrazole core), pyrazole-bridged CA4 analogs reported and there has not been a systematic evaluation into the effect of substitution pattern. The pyrazole motif is an important fragment in the pharmaceutical industry and is present in a number of commercial medicines and agrichemicals.[29,30] However, synthetic routes to these structurally important diazoles are often linear or suffer from regioselectivity issues during the heterocycle forming step. In this regard, we felt that sydnones could represent convenient and potentially versatile starting materials to access these desirable therapeutic analogs. Sydnones belong to the mesoionic family of compounds and they undergo [3+2] cycloaddition-retrocycloaddition reactions with alkynes to form pyrazoles.[31] These cycloadditions can be highly regioselective and offer access to a wide range of pyrazoles.[32,33,34,35,36,37] In the context of developing novel VDAs, we envisaged that the sydnone cycloaddition strategy could be exploited to access a broad range of pyrazole templated combretastatin analogs from similar starting materials (*Scheme 1*). However, we recognized that a number of synthetic challenges needed to be met in order to achieve this goal: (1) access to 1,5-substituted pyrazoles theoretically required high temperature cycloaddition with acetylene gas; (2) 4,5-disubstituted pyrazoles required the innate regioselectivity of the cycloaddition with terminal alkynes to be reversed (typically, the largest substituent is incorporated at the *C*3); (3) the cycloaddition of

biaryl alkynes for the preparation of 3,4-substituted pyrazoles was unlikely to proceed with regiocontrol, thereby delivering isomeric mixtures.

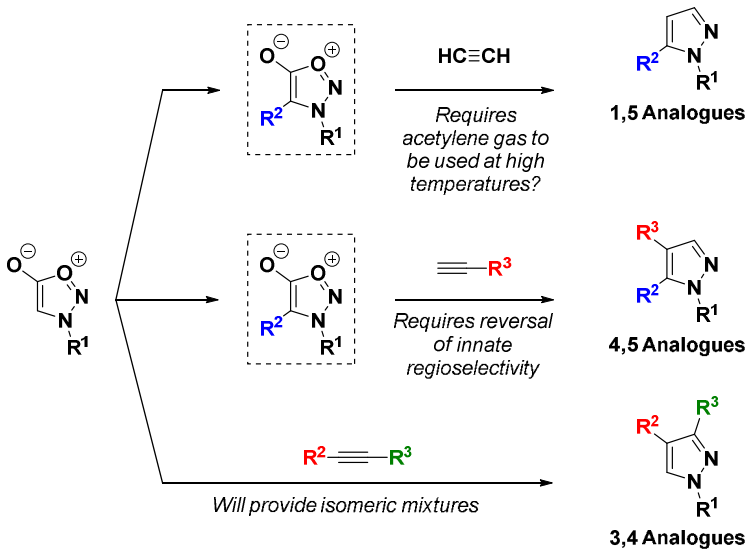

Scheme 1. Sydnone cycloaddition strategy to pyrazole-based analogs

Results and Discussion

Preparation of 1,5-Disubstituted Analogs

Our investigations began with the preparation of 1,5-disubstituted pyrazoles. We proposed a strategy that exploited our previously developed direct arylation of sydnones to furnish the key diaryl intermediates (*Scheme 2*).[38] We then envisaged that trimethylsilylacetylene could act as a high-boiling point acetylene equivalent in the cycloaddition to provide the target pyrazoles after protodesilylation.

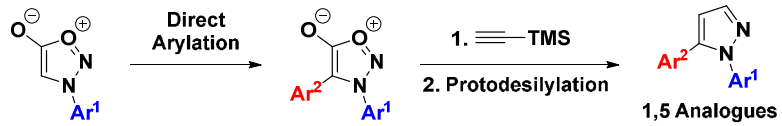

Scheme 2. Strategy for the synthesis of 1,5-disubstituted pyrazoles

Sydnone starting materials were readily prepared by established routes of *N*-nitrosation of amino acids, followed by cyclodehydration with trifluoroacetic anhydride (TFAA).[31,38] The synthesis began with the coupling of sydnone **1** affording diaryl sydnone **2** in moderate yield (*Scheme 3*). Pleasingly, sydnone **2** underwent successful cycloaddition with trimethylsilylacetylene to afford TMS-substituted pyrazoles **3a** and **3b** in good yield and excellent (but inconsequential) regioselectivity. Previous experience had suggested that 3-silyl pyrazoles could be particularly resistant to hydrolysis. Fortunately however, a refluxing solution of TBAF in THF afforded the desilated product **4** in useful yield. Finally, simple hydrogenation of the benzyl ether afforded CA4 analog **5**.

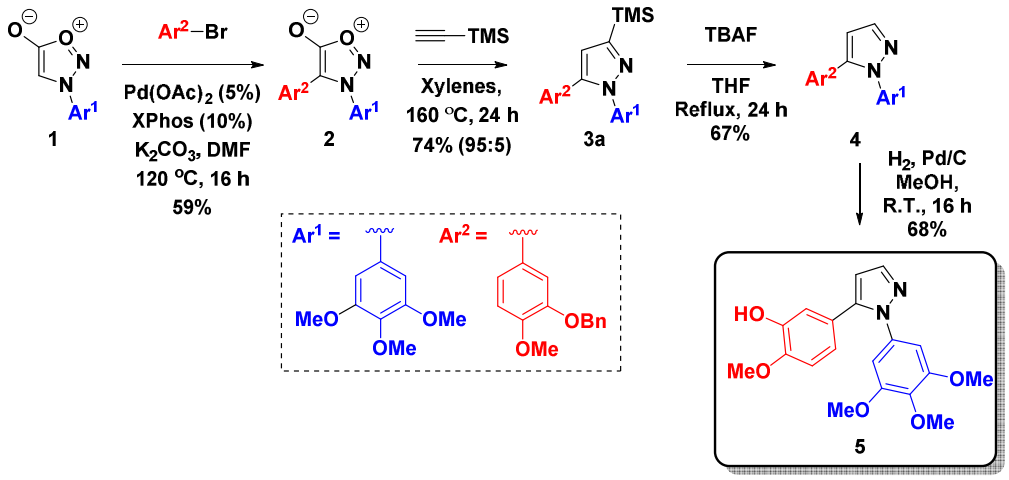

Scheme 3. Synthesis of pyrazole **5**

Preparation of the isomeric 1,5-pyrazole **10** required a slight modification to the route. Sydnone **6** was subjected to direct arylation conditions, followed by benzyl protection of the phenol (*Scheme 4*). Surprisingly, benzyl protection of the phenol prior to direct arylation resulted in a sydnone that decomposed when subjected to various direct arylation conditions. Sydnone **7** underwent cycloaddition in very good yield and regioselectivity. TBAF deprotection of the trimethylsilyl group proceeded in moderate yield. The resulting pyrazole

9 was contaminated with a small amount of an inseparable, unknown by-product. Fortunately, analog **10** was isolated cleanly after benzyl hydrogenation.

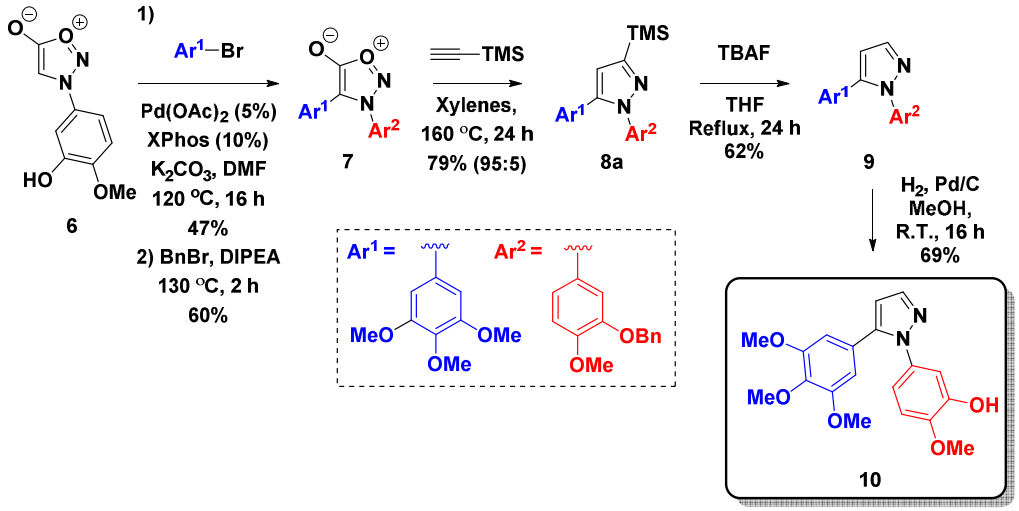

Scheme 4. Synthesis of pyrazole **10**

Preparation of 4,5-Disubstituted Analogs

We next turned our attention to the preparation of 4,5-disubstituted pyrazoles. Elegant work by Taran *et al.* demonstrated that copper catalysis can reverse the natural regioselectivity of sydnone cycloadditions.[33] Recently, the chemistry has been improved to tolerate bromide substituents at the sydnone *C*4 position, which could then be further elaborated by cross-coupling.[32] However, this chemistry is currently limited to *N*-aryl sydnones. As our interest lay with *N*-alkyl sydnones, a new methodology was needed. We proposed to extend the strategy used for the synthesis of 1,5-substituted pyrazoles to borylated trimethylsilylacetylene (*Scheme 5*). We have previously reported the cycloaddition of alkynylboranes with sydnones to be highly regioselective and importantly, tolerant of *N*-alkylsydnones.[35] In the case of disubstituted alkynes, the boron substituent is generally incorporated at the pyrazole *C*4 position.

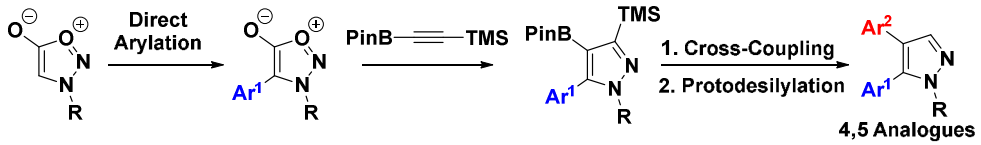

Scheme 5. Strategy for the synthesis of 4,5-disubstituted pyrazoles

The synthesis began with the direct arylation of *N*-methyl- and *N*-benzylsydnone, which proceeded smoothly on gram scale affording *C*4-arylated sydnones **11-14** (*Scheme 6*). We were delighted to find all substrates successfully underwent cycloaddition and the corresponding pyrazoles were isolated as single regioisomers, **15-18**, albeit contaminated with varying amounts of protodeborylated by-product. The Suzuki-Miyaura reaction required some optimization, but was successfully achieved using Buchwald's XPhosPdG2 precatalyst to afford **19-22**. The products were again contaminated with varying amounts of protodeborylated by-product. Pleasingly, subjection of **23-26** to refluxing TBAF successfully resulted in silyl deprotection, and **23-26** were readily separable from their corresponding by-products at this stage. Benzyl hydrogenation afforded the 4,5-disubstituted analogs of CA4, **27-32**. In the case of *N*-benzylpyrazoles **24** and **26**, incomplete hydrogenation afforded a separable mixtures of *N-H* pyrazoles **28** and **31** and *N*-benzylpyrazoles **29** and **32** respectively.

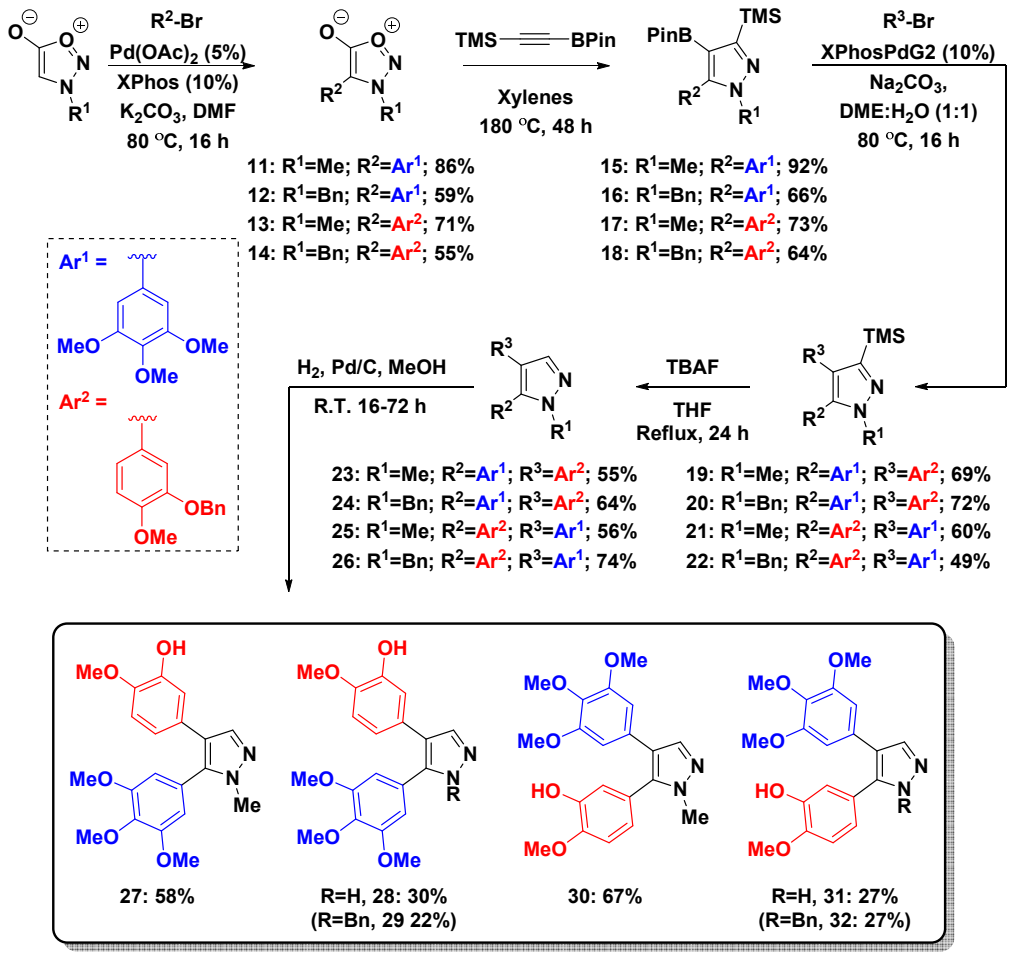

Scheme 6. Synthesis of 4,5-disubstituted analogs

Preparation of 3,4-Disubstituted Analogs

The final analogs to prepare were the 3,4-disubstituted pyrazoles. It was originally anticipated that we could utilize alkynylboronate cycloaddition chemistry to access these compounds (*Scheme 7, A*).[36] However, we found that alkynes bearing these particularly electron rich aromatic rings were prone to protodeborylation, and pyrazole boronic esters could not be obtained under a variety of conditions. We proposed an alternative route whereby the innate regioselectivity of the sydnone cycloaddition was exploited, followed by bromination and subsequent cross-coupling (*Scheme 7, B*).

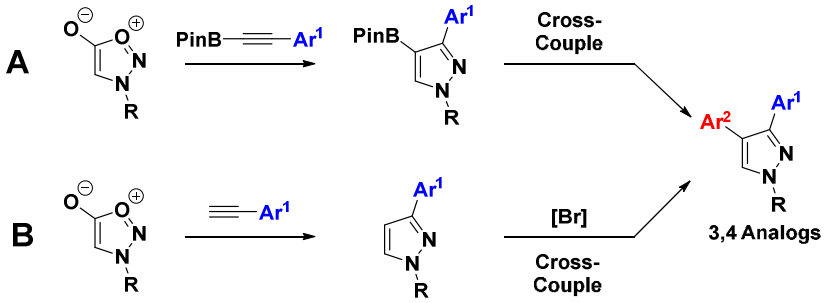

Scheme 7. Strategy for the synthesis of 3,4-disubstituted pyrazoles

The route began with the cycloaddition of *N*-methyl and *N*-benzylsydnone with arylacetylenes. The reactions proceeded in good yield and high regioselectivity to afford pyrazoles **33-36** (*Scheme 8*). We were pleased to find that *N*-bromosuccinamide (NBS) in acetonitrile rapidly and selectively brominated the pyrazoles. After basic work-up, the brominated products could be subjected without further purification to Suzuki-Miyaura coupling, affording products **37** and **39** in good yield over 2 steps. Products **38** and **40** were isolated after subjection of the crude Suzuki-Miyaura products to silyl deprotection conditions of potassium carbonate in refluxing methanol in useful yield over 3 steps. In the case of *N*-methyl analogs **37** and **39**, this route represents rapid access to the compounds in effectively 2 pots. Compounds **38** and **40** were subjected to hydrogenation to afford the free *NH*-pyrazole analogs **28** and **31**, thus providing an alternative, shorter route to these analogs from the alkynylboronate strategy above.

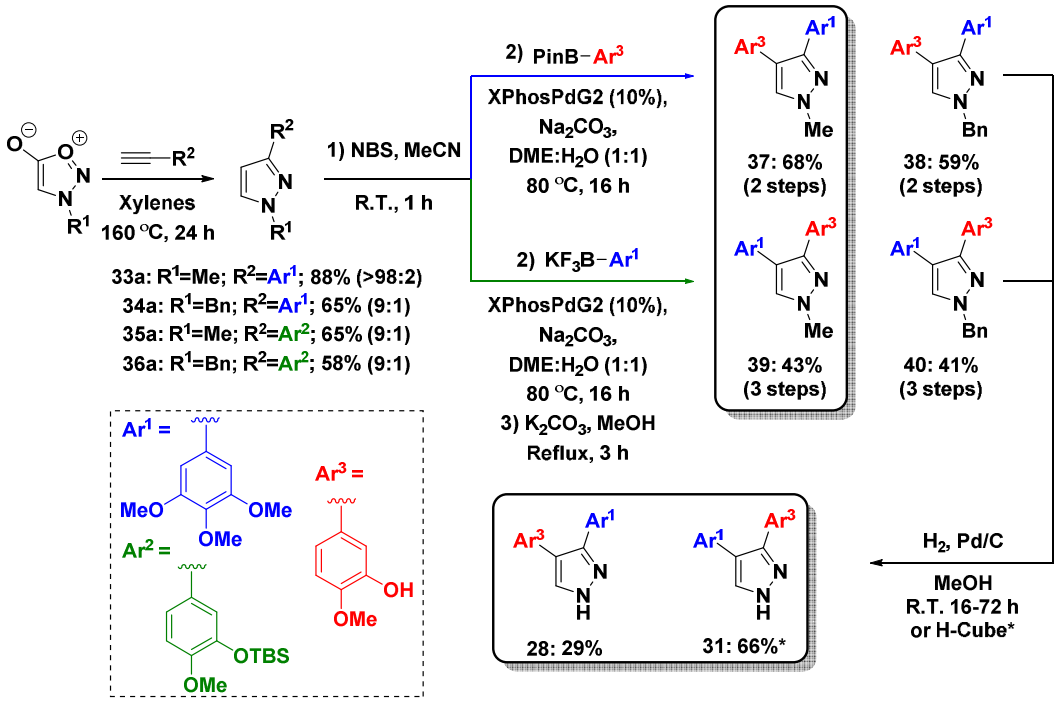

Scheme 8. Synthesis of 3,4-disubstituted analogs

Biological Evaluation

With a library of twelve pyrazole-based analogs of CA4 in hand, attention turned to evaluating their potential as anticancer agents. Studies within our laboratories have previously shown that for CA4P, vascular disruptive effects dominate rather than direct targeting of cancerous cells.[39] Therefore, we proposed that the primary target of VDAs, endothelial cells, would provide an accurate insight into the activity of the pyrazole-based analogs.

Initial Screens

CA4 is a tubulin binding agent, therefore we proposed that a convenient method for the rapid assessment of activity was to study the effects of compounds on endothelial cell proliferation, which is inhibited by disruption of the microtubule-rich mitotic spindle. It is important to note that the action of CA4 as a VDA is not due to effects on HUVEC proliferation or

prevention of mitotic spindle formation. However, the analysis of drug-induced effects cell proliferation provide a useful insight into microtubule targeting potential. Screening results are depicted in Table 1.

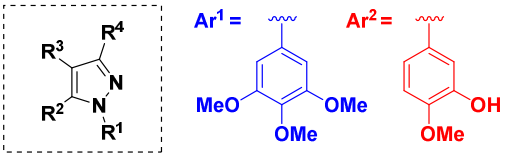

Entry	Compound	R^1	R^2	R^3	R^4	GI_{50}
1	**5**	Ar^1	Ar^2	H	H	28 nM
2	**10**	Ar^2	Ar^1	H	H	>750 nM
3	**27**	Me	Ar^1	Ar^2	H	68 nM
4	**28**	H	Ar^1	Ar^2	H	>5000 nM
5	**29**	Bn	Ar^1	Ar^2	H	>2500 nM
6	**30**	Me	Ar^2	Ar^1	H	118 nM
7	**31**	H	Ar^2	Ar^1	H	7 nM
8	**32**	Bn	Ar^2	Ar^1	H	>750 nM
9	**37**	Me	H	Ar^2	Ar^1	>5000 nM
10	**38**	Bn	H	Ar^2	Ar^1	>5000 nM
11	**39**	Me	H	Ar^1	Ar^2	256 nM
12	**40**	Bn	H	Ar^1	Ar^2	>2000 nM
13	CA4P	-	-	-	-	8 nM
14	Colchicine	-	-	-	-	25 nM

Table 1. Values for growth inhibition of HUVECs by pyrazole anologs vs. CA4P and colchicine

The variation observed in the activities of the compounds was quite remarkable given that all of the compounds screened were direct analogs of CA4, differing only in their location on the

pyrazole core. The most active compounds **5**, **27**, **30** and **31** (*entries 1, 3, 6 and 7*) exhibited low nanomolar activity. The most active compound **31**, showed similar activity to CA4P (*entry 7 vs 13*). However, a number of compounds only showed low micromolar activities (*entries 4, 9 and 12*). Further studies were undertaken on the two most active compounds **5** and **31** (*Figure 2*).

Immunofluorescence Studies

To confirm that the drug effects were due to microtubule disruption, drug-induced changes in the endothelial cell cytoskeleton and morphology were studied *via* immunofluorescence for compounds **5** and **31**. The microtubule disruption associated with CA4P treatment is also accompanied by changes in cell shape and morphology brought about by the rapid remodelling of the actin cytoskeleton.[40] Therefore, endothelial cells in culture were stained for actin filaments using phalloidin, microtubules using an antibody to β–tubulin and nuclei stained with 4',6-diamidino-2-phenylindole (DAPI).

In cells that are in interphase, polymers of α–tubulin and β–tubulin originate from the centrosome and radiate to the edge of the cell as tubular filaments referred to as microtubules (*Figure 3, A*), whereas actin is mostly pericellular (*Figure 3, B*). Upon treatment with 250 nM CA4P for 30 minutes, interphase microtubules became disrupted (*Figure 3, C*), leading to changes in cell morphology. Disruption of microtubules led to the formation of actin stress fibres across the cells (*Figure 3, D*). Interestingly, a longer (90 minutes) treatment at a higher dose of 1 μM was required for similar effects to be observed with colchicine (*Figure 3, E and F*). A 250 nM treatment with **5** resulted in the disruption of interphase microtubules and significant changes in endothelial cell shape and morphology (*Figure 3, G and H*). Similarly, a 250 nM treatment with **31** also caused pronounced effects on endothelial cell shape and morphology (*Figure 3, I and J*).

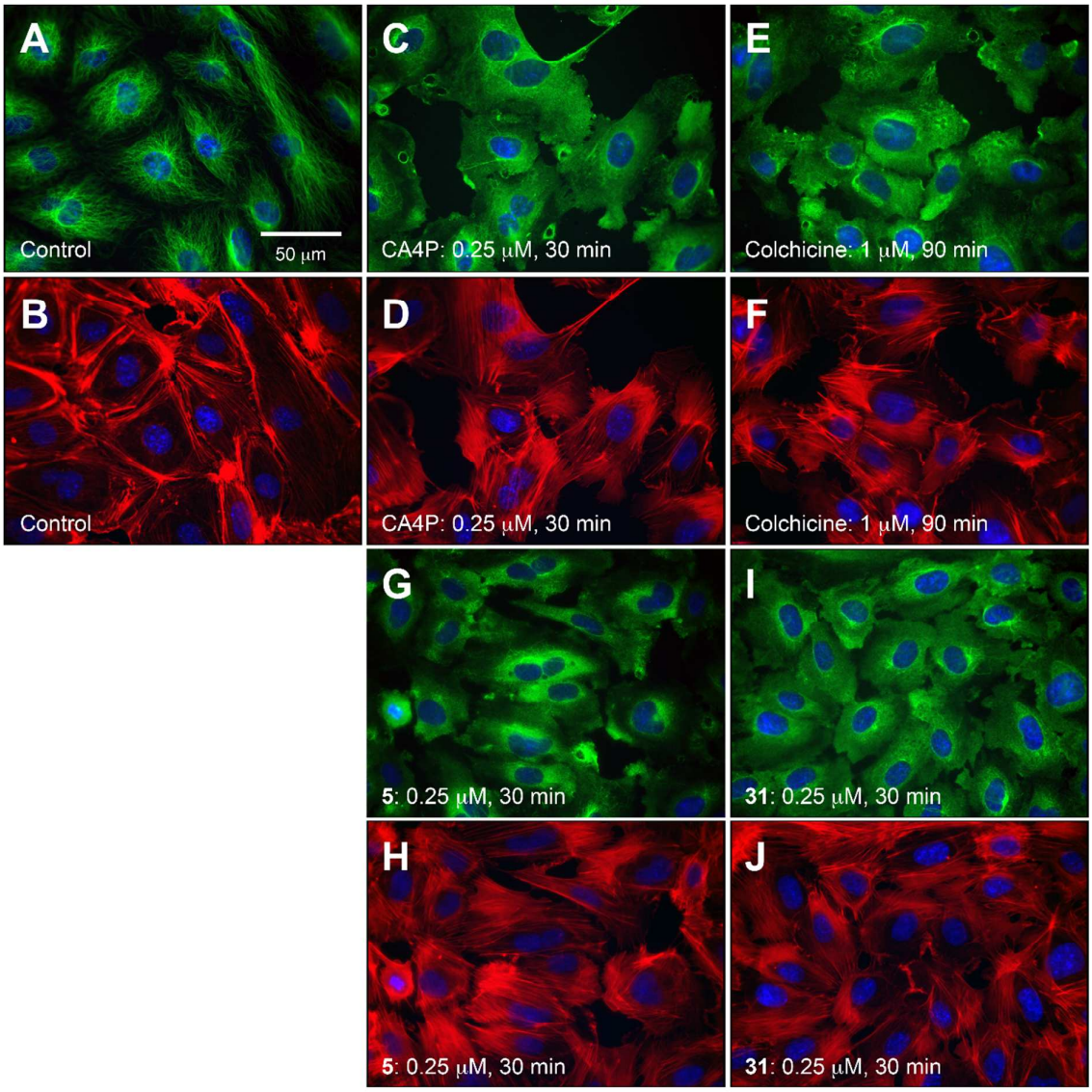

Figure 3. Drug effects on HUVEC cytoskeletal structures. Cells were treated with a single dose of either vehicle (A, B), 250 nM CA4P (C, D), 1 μM colchicine (E, F), 250 nM drug **5** (G, H) or 250 nM drug **31** (I, J). Drug treatments were for 30 min with CA4P, drug **5** and drug **31** and 90 minutes with colchicine. Cells were fixed and stained with an antibody to β-tubulin (A, C, E, G, I) and F-actin (B, D, F, H, J) and nuclei stained with DAPI.

Recovery Experiments

CA4P is thought to be a potent VDA at well below its maximum tolerated dose due to the reversibility of its binding to tubulin.[12] Therefore, we tested the reversibility of the tubulin binding of compounds **5** and **31** using immunofluorescence in parallel with CA4P and colchicine.

As shown in Figure 3, a 30 minute treatment with 250 nM of either CA4P, **5** or **31** was sufficient to produce a profound effect on cellular morphology. A 30 minute treatment with CA4P, followed by removal of the drug and 60 minutes incubation led to significant recovery of the cells *(Figure 4, A and B).* There was a clear recovery of microtubules and a reduction in actin stress fibres. Importantly, cells treated with colchicine did not show signs of recovery within the same time frame (*Figure 4, C and D*). Indeed, recovery was not observed, even after a 120 minute incubation upon removal of the drug (*Figure 4, E and F*). Our interpretation of these data is as follows. Firstly, that the binding of colchicine was indeed pseudo-irreversible whereas CA4 bound reversibly, and secondly that its action was slower than that of CA4. It is also interesting to note that this slower action was not due to a decreased rate of diffusion through the cell membrane. If it were the case, removal of the drug after thirty minutes would prevent microtubule disruption. Furthermore, **5** appeared to have a similar profile to CA4P with the cells also showing full recovery after 60 minutes (*Figure 4, G and H*). Intriguingly, cells treated with **31** did not recover significantly 60 minutes after drug removal (*Figure 4, I and J*). However, early signs of recovery were apparent at this time point, because microtubules were beginning to radiate from the centrosome (*I*). Full recovery of the cytoskeleton was nevertheless seen 120 minutes after drug removal (*Figure 4, K and L*). This slower recovery than CA4P was particularly interesting because we felt it could be an indicator to either a wider therapeutic window or toxicity. Either result would add value to this assay in assessing the viability of compounds as

VDAs *in vitro*. Such a model has been quite elusive thus far. Therefore, we sought to further probe the potential of **31** as a VDA.

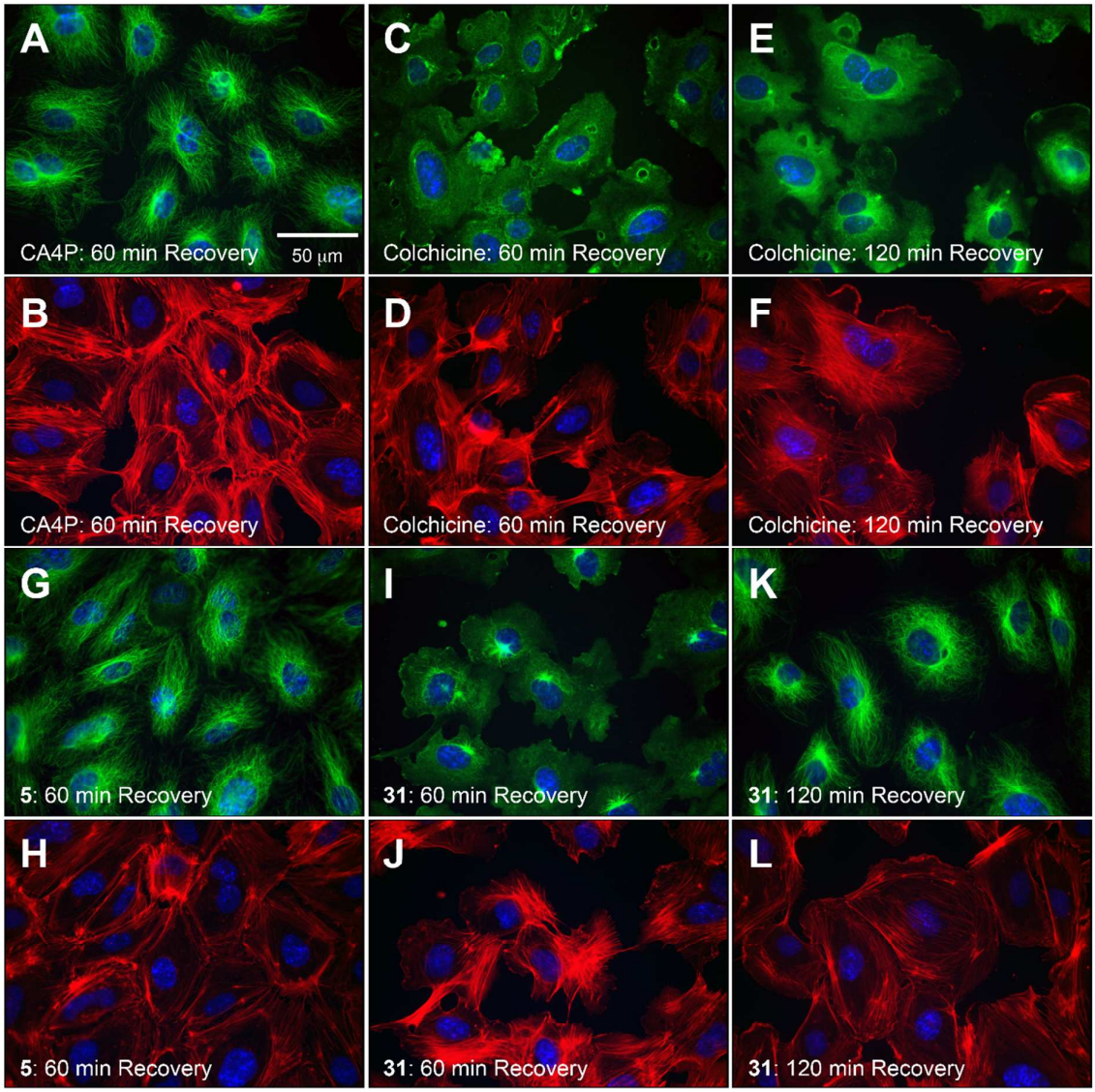

Figure 4. Recovery of cytoskeletal structures after drug removal. HUVECs were treated with a single dose of either 250 nM CA4P (A, B), 1 μM colchicine (C, D, E, F), 250 nM drug **5** (G, H) or 250 nM drug **31** (I, J, K, L). Drug treatments were for 30 min. Cells were then washed with serum containing medium and allowed to recover for 60 min (A, B, C, D, G, H, I, J) or 120 min (E, F, K, L). Cells were fixed and stained with an antibody to β-tubulin (A, C, E, G, I, K) and F-actin (B, D, F, H, J, L) and nuclei stained with DAPI.

Analysis of Rho-GTPase/Rho Kinase Signalling Pathway Activation.

We focused on the most active compound from the initial screens, **31** and compared its activity to CA4P in assays linked to mode of action and vascular disruption. Previous studies had revealed that activation of the RhoA-GTPase signal pathway was involved in actin remodelling and monolayer disruption caused by CA4P.[40,41] Activated Rho-GTPase causes contractility and stress fibre formation through polymerization of actin and the phosphorylation of myosin light chain (MLC). The latter activity is dictated through the activation of serine/threonine Rho kinases (ROCKs). Thus, we investigated both **31** and CA4P induced effects on the phosphorylation of MLC (pMLC) in HUVECs. As shown in Figure 5, both compounds instigated significant increases in pMLC over a range of concentrations, indicating that both compounds were acting *via* a similar pathway. Compound **31** induced significant phosphorylation of MLC at the lower tested concentration of 50 nM while CA4P was less active at this dose. To further confirm the involvement of ROCK in the induction of MLC phosphorylation by compound **31**, cells were treated with the specific ROCK inhibitor Y-27632. Similar to what was previously published for CA4P,[40,41] the induction of MLC phosphorylation by compound **31** was abrogated by Y-27632, confirming the involvement of ROCK in this process (*Figure 5C*).

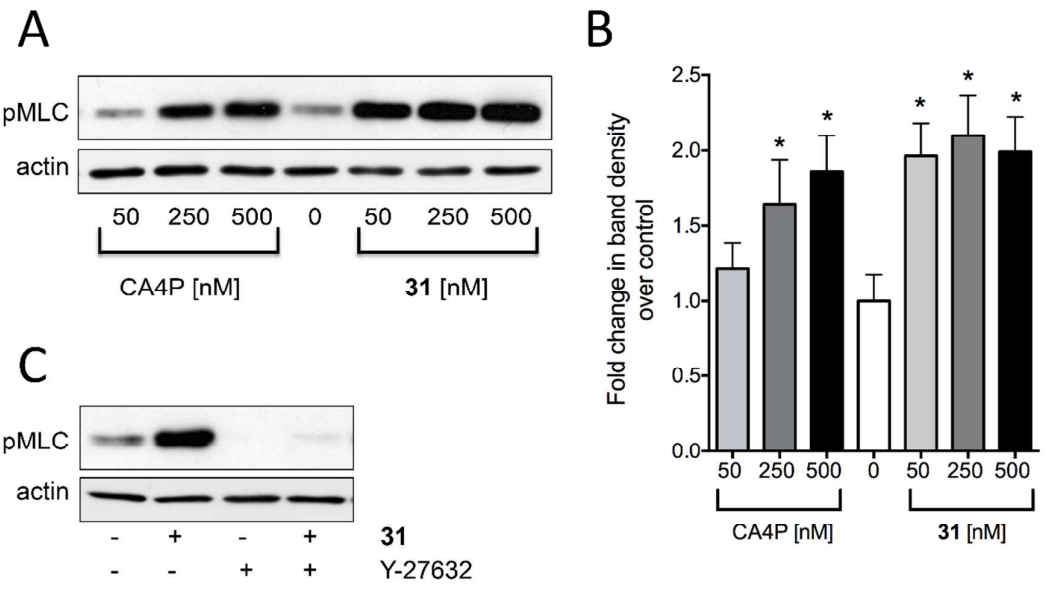

Figure 5. Drug-induced induction of phosphorylation of Rho kinase target MLC. HUVECs were treated with increasing concentrations of CA4P or drug **31** for 15 minutes after which proteins were extracted and analyzed for phosphorylation of ROCK target MLC (pMLC) by western blotting using an antibody specific to the phosphorylated form of the protein (A). Immunoblots were reprobed with an antibody to actin to confirm equal loading. In B, pMLC band intensities were analyzed by ImageJ and results expressed as fold-change over control cells treated with vehicle alone. Each column represents the mean of 3-4 independent cell culture experiments±SEM. * represents $P < 0.05$ for the significance of differences between drug treatment groups and controls (one-way ANOVA followed by a Tukey post-test). In C, HUVECs were incubated with Rho kinase inhibitor Y-27632 (5 μM) for 5 minutes and then treated with 500 nM drug **31** for 15 minutes. Proteins were extracted and analyzed for pMLC as in A.

Endothelial Monolayer Permeability Experiments

Rapid disruption of the endothelial cell monolayer is key to the activity of VDAs.[40] Therefore, studies on the effects of compound **31** and CA4P on cell monolayer permeability

to fluorescent dextran were undertaken. Confluent HUVEC monolayers were treated for 30 minutes before removal of the drug and addition of fluorescent dextran for a further 30 minutes. Since **31** was shown above to be effective at triggering induction of Rho signalling at a concentration of 50 nM (see Figure 5), both CA4P and compound **31** were tested at this dose. Both drugs instigated a significant increase in monolayer permeability at this low dose (*Figure 6*). Importantly however, **31** led to a significantly larger increase in monolayer permeability than CA4P at this dose. This correlated with the increased activity of compound **31** over CA4P in stimulating pMLC phosphorylation.

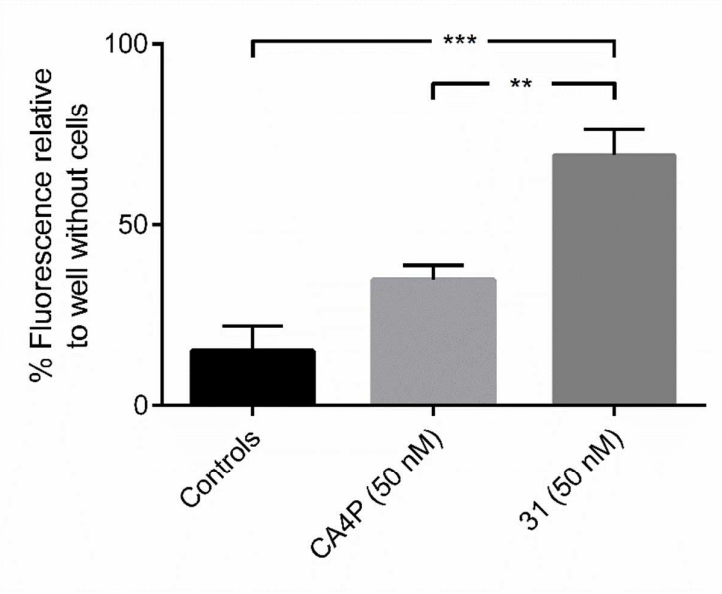

Figure 6. Drug-induced changes in endothelial monolayer permeability comparing CA4P and **31**. Confluent monolayers of cells grown on microporous filter inserts were treated with vehicle control, CA4P (50 nM, 30 min) or compound **31** (50 nM, 30 min). Drugs were removed and replaced with FITC–dextran for a further 30 min. The passage of FITC-dextran through the monolayer was quantified and expressed as a percentage of FITC that passed through a filter without cells. Results are a mean of 3 independent experiments ± SEM. ** represents $P < 0.01$ and *** represents $P < 0.001$ for the significance of differences between groups (one-way ANOVA followed by a Tukey post-test).

In Vivo Studies

The maximum tolerated dose (MTD) of **31** in SCID (severe combined immunodeficiency) mice was found to be greater than 162 mg/kg (0.454 mmol/kg; data not shown). We next investigated whether **31** showed efficacy in a tumor model. SCID mice were implanted with 5 x 10^6 SW1222 (human colorectal adenocarcinoma) cells *via* subcutaneous injection. Tumors were allowed to reach 8 mm in diameter and then treated with either vehicle (50% Na_2CO_3/NaCl), CA4P (100 mg/kg, 0.227 mmol/kg) or a solution of **31** (81 mg/kg, 0.227 mmol/kg). Tumors were excised 24 hours later and necrosis levels calculated in H&E stained 5 μm thick sections by a random point scoring microscopy method using a 'Chalkley' eyepiece graticule.[42,43] As shown in Figure 7, CA4P treated tumors were significantly more necrotic than the untreated tumors, with % necrosis very similar for CA4P and **31** treated tumors. However, the tendency for necrosis to increase with **31** treatment just failed to reach significance with the animal numbers used (*Figure 7*). CA4P appeared to exhibit greater variability in necrosis levels with some tumors showing no response upon treatment. Maximum response was higher for CA4P, but over one third of the treatment group failed to respond. In contrast, treatment with **31** resulted in much less variation, with 11% (a single tumor) failing to respond. It is of particular note that **31** showed signs of efficacy *in vivo* without further derivatisation for water solubility and appeared to remain active in the circulation.

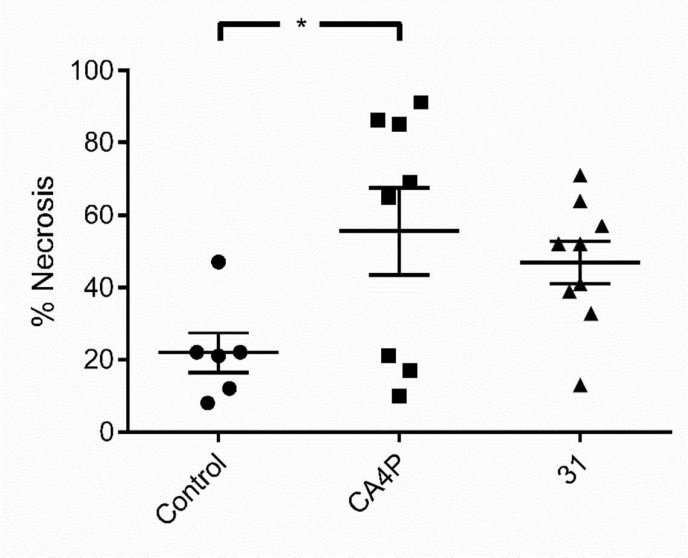

Figure 7. *In vivo* study of drug-induced effects on tumor cell necrosis comparing CA4P and **31**. Each point represents the combined data from a single tumor. 5 sections (cut at different tumor depths) were analyzed per tumor using a x20 objective on a Nikon Eclipse TS100 microscope microscope. The total section was analyzed and % necrosis calculated in each field from the relative number of points in a Chalkley eyepiece graticule co-incident with necrotic versus viable tumor tissue. Bars represent the mean±SEM of the combined data for each tumor. * represents $P < 0.05$ for the significance of differences between groups (one-way ANOVA followed by a Tukey post-test).

Conclusion

In conclusion, we have successfully utilized highly-regioselective cycloadditions of sydnones to access twelve direct pyrazole-based analogs of combretastatin A4. Two of the compounds display similar efficacy to CA4P *in vitro*. We have established that both compounds exhibit reversible binding and that the most active compound activates the RhoA-ROCK pathway, a characteristic of a CA4P-like mode of action. The most active compound also significantly increases cell monolayer permeability relative to CA4P at doses of 50 nM. Finally, evaluation of compound efficacy *in vivo* showed a tendency toward increased necrosis in a similar

manner to CA4P at an equivalent dose, without the need for the incorporation of water solubilizing groups.

Experimental

^{1}H NMR spectra were recorded on a Bruker AVIII HD 400 (400 MHz), Bruker AVI 400 (400 MHz), or DPX-400 (400 MHz) supported by an Aspect 3000 data system. Chemical shifts are reported in parts per million (ppm) from tetramethylsilane with the residual protic solvent resonance as the internal standard ($CHCl_3$: δ 7.26, DMSO: δ 2.50). ^{13}C NMR spectra were recorded on a Bruker AVIII HD 400 (100.6 MHz), Bruker AVI 400 (100.6 MHz), or DPX-400 (100.6 MHz) with complete proton decoupling. Chemical shifts are reported in ppm from tetramethylsilane with the solvent as the internal reference ($CDCl_3$: δ 77.16, DMSO: δ 39.52). High-resolution mass spectra (HRMS), recorded for accurate mass analysis, were performed on electrospray mode (TOF ES+). Infrared (IR) spectra were recorded on a Perkin Elmer Paragon 100 FTIR spectrophotometer, νmax in cm^{-1}. Samples were recorded as solids using a solid probe. Bands were characterised as broad (br), strong (s), medium (m), and weak (w). All solvents and reagents obtained from Acros, Fisher, Sigma, Alfa or Fluorochem and used without purification unless specified. Flash chromatography was performed on silica gel (BDH Silica Gel 60 43-60). Thin layer chromatography (TLC) was performed on aluminium backed plates pre-coated with silica (0.2 mm, Merck DC-alufolien Kieselgel 60 F254) which were developed using ultraviolet (UV). HPLC chromatograms were obtained on a Perkin Elmer Series 200 HPLC system using a Waters XBridge C18 250 x 4.6 mm column and a gradient of 5-95% MeCN/H_2O over 20 min. All compounds submitted for biological testing were recrystallized to consistent melting point and judged as >95% pure by HPLC and ^{1}H and ^{13}C NMR spectroscopy.

N-Methyl-, *N*-benzyl- and *N*-(3,4,5-trimethoxyphenyl)sydnone (**1**)[38] were prepared by standard methods (cyclodehydration of *N*-nitroso amino acid with trifluoroacetic anhydride) similarly to *N*-(3-hydroxy-4-methoxyphenyl)sydnone (see below).

General Procedure A: Direct Arylation of Sydnones. A mixture of sydnone (1 eq.), aryl halide (1.5 eq.), palladium acetate (5 mol %), XPhos (10 mol %) and potassium carbonate (2-3 eq.) in DMF (0.1 – 0.5 M) under an atmosphere of nitrogen was heated at 80 - 120 °C for 14 hours before the reaction was allowed to cool to ambient temperature and water was added. The resulting mixture was extracted with ethyl acetate:40-60 petroleum ether (9:1) and the combined organic layers dried over $MgSO_4$ and concentrated *in vacuo*. Flash silica chromatography (eluting solvent 20%-100% ethyl acetate in 40-60 petroleum ether) afforded the target 3,4-disubstituted sydnones. The compounds could be further purified by recrystallization from ethanol or dichloromethane/petrol.

General Procedure B: Cycloaddition of Sydnones with Terminal Alkynes.

A Schlenk tube was charged with sydnone (1 eq.), alkyne (2-4 eq.) and xylenes (1 M). The tube was then sealed and heated at 160 ^{o}C for 24 hours. The mixture was allowed to cool to ambient temperature and loaded onto a short plug of silica and washed with 40-60 petroleum ether before elution with ethyl acetate. Volatiles were removed *in vacuo* and the crude residue purified by flash silica chromatography (gradient starting with 100% 40-60 petroleum ether and ending with 40% ethyl acetate in 40-60 petroleum ether) affording the target trisubstituted pyrazoles as mixtures of regioisomers. Only characterization for the major regioisomer is reported.

General Procedure C: Preparation of Pyrazole Boronic Esters. A Schlenk tube was charged with sydnone (1 eq.), alkyne (2 eq.) and xylenes (1 M). The tube was then sealed and heated at 180 ^{o}C for 48 hours. The mixture was allowed to cool to ambient temperature and

loaded onto a short plug of silica and washed with 40-60 petroleum ether before elution with ethyl acetate. Volatiles were removed *in vacuo* and the crude residue purified by flash silica chromatography (gradient starting with 100% 40-60 petroleum ether and ending with 40% ethyl acetate in 40-60 petroleum ether) affording the target pyrazole boronic esters as an inseparable mixture of the target material and the product arising from protodeboronation. Only characterization for the target material is reported. ^{13}C NMR signals for C-B were not observed due to T_2 broadening.

General Procedure D: Suzuki-Miyaura Coupling of Pyrazole Boronic Esters. A flask equipped with a reflux condenser was charged with pyrazole boronic ester (1 eq.), XPhosPdG2 (0.1 eq.), sodium carbonate (2 eq.) and degassed 1,2-dimethoxyethane:water (1:1, 0.1 M) and heated at 80 ^{o}C under an inert atmosphere of nitrogen for 14 hours. The mixture was allowed to cool to ambient temperature, poured into water and extracted with ethyl acetate. The combined organic layers were dried over $MgSO_4$ and concentrated *in vacuo*. Flash silica chromatography (gradient starting with 100% 40-60 petroleum ether and ending with 40% ethyl acetate in 40-60 petroleum ether) afforded the target cross-coupled pyrazoles as an inseparable mixture of the target material and the product arising from protodeboronation. Only characterization for the target material is reported.

General Procedure E: Trimethylsilyl Group Cleavage. A flask equipped with a reflux condenser was charged with pyrazole (1 eq.), and TBAF (10 eq. 1 M solution in THF) and heated at reflux under an inert atmosphere of nitrogen for 24 hours. The mixture was allowed to cool to ambient temperature, poured into water, neutralized with $NaHCO_3$ and extracted with ethyl acetate. The combined organic layers were dried over $MgSO_4$ and concentrated *in vacuo*. Flash silica chromatography (gradient starting with 100% 40-60 petroleum ether and ending with 60% ethyl acetate in 40-60 petroleum ether) afforded the target desilated pyrazoles.

General Procedure F: Bromination and Subsequent Suzuki-Miyaura Coupling of Pyrazoles. i) To a flask containing pyrazole was added a solution of *N*-bromosuccinamide (1 eq.) in acetonitrile (0.2 M). The resulting mixture was stirred for one hour at ambient temperature, before being poured into water. The mixture was extracted with ethyl acetate and the combined organic layers washed with aqueous sodium hydroxide (1 M). The organic layer was dried over $MgSO_4$, filtered and volatiles removed *in vacuo*. The crude material was concentrated into a flask. The flask was then charged with aryl boronate (1.5 eq.), XPhosPdG2 (10 mol %), sodium carbonate (2-3.5 eq.) and thoroughly degassed 1,2-dimethoxyethane:water (1:1, 0.1 M). The mixture was heated at 80 ^{o}C for 14 hours, cooled to ambient temperature, poured into water and extracted with ethyl acetate. The combined organic layers were dried over $MgSO_4$, filtered and volatiles removed *in vacuo*. Flash silica chromatography (gradient starting with 100% 40-60 petroleum ether and ending with 100% ethyl acetate in 40-60 petroleum ether) afforded the target pyrazoles. **ii)** In cases where the products obtained were the TBS-protected phenols, the crude Suzuki product was subjected to potassium carbonate (3 eq.) in refluxing methanol for 3 hours, before the mixture was poured into water and extracted with ethyl acetate. The organic layers were dried over $MgSO_4$, filtered and volatiles removed *in vacuo*, followed by purification.

General Procedure G: Benzyl Deprotection. A flask was charged with pyrazole and Pd/C (10% wt./wt., 100 mg/mmol) and methanol (0.1 M). The flask was flushed with H_2 (balloon) and stirred for 24-72 hours. The mixture was filtered through celite^{TM} and concentrated *in vacuo*. Flash silica chromatography (gradient starting with 100% 40-60 petroleum ether and ending with 100% ethyl acetate in 40-60 petroleum ether) afforded the target debenzylated pyrazoles.

4-(3-Phenylmethoxy-4-methoxyphenyl)-*N*-(3,4,5-trimethoxyphenyl)sydnone (2). *N*-3,4,5-Trimethoxyphenylsydnone (500 mg, 1.98 mmol) and 1-bromo-3-phenylmethoxy-4-

methoxybenzene (872 mg, 2.97 mmol) were subjected general procedure A, affording **2** as a colourless solid (542 mg, 59%). M.p.: 144-146 °C; ^{1}H NMR (400 MHz, $CDCl_3$) δ 3.78 (6H, s), 3.87 (3H, s), 3.92 (3H, s), 4.97 (2H, s), 6.64 (2H, s), 6.81 (1H, d, *J* = 8.5 Hz), 6.92 (1H, dd, *J* = 8.5, 2.0 Hz), 6.98 (1H, d, *J* = 2.0 Hz), 7.27-7.35 (5H, m); ^{13}C NMR (101 MHz, $CDCl_3$) δ 56.1, 56.7, 61.3, 71.0, 102.6, 108.0, 111.8, 112.6, 117.0, 120.9, 127.8, 128.1, 128.7, 130.0, 136.6, 140.7, 148.2, 150.2, 154.2, 167.1; FTIR: ν_{max} 2939 (w), 1738 (m), 1602 (m), 1260 (s), 1234 (s), 1132 (s), 1016 (m), 993 (m); HRMS (ESI-TOF) *m/z* $[M+H]^+$ calculated for $C_{25}H_{25}N_2O_7$: 465.1656. Found: 465.1654.

1-(3,4,5-Trimethoxyphenyl)-3-(trimethylsilyl)-5-(3-phenylmethoxy-4-methoxyphenyl)-pyrazole (3a, major) and 1-(3,4,5-trimethoxyphenyl)-4-(trimethylsilyl)-5-(3-phenylmethoxy-4-methoxyphenyl)-pyrazole (3b, minor). Sydnone **2** (136 mg, 0.293 mmol) and trimethylsilylacetylene (115 mg, 1.17 mmol) were subjected to general procedure B, affording an inseparable mixture of pyrazoles **3a** and **3b** as an orange oil (113 mg, 75%, 95:5). ^{1}H NMR (400 MHz, $CDCl_3$) δ 0.36 (9H, s), 3.69 (6H, s), 3.82 (3H, s), 3.87 (3H, s), 4.95 (2H, s), 6.51 (1H, s), 6.52 (2H, s), 6.76 (1H, d, *J* = 1.5 Hz), 6.81-6.88 (2H, m), 7.24-7.35 (5H, m); ^{13}C NMR (101 MHz, $CDCl_3$) δ -0.9, 56.0, 56.1, 61.0, 71.1, 103.3, 111.5, 113.4, 114.6, 122.0, 123.3, 127.0, 127.9, 128.6, 136.1, 136.8, 137.3, 142.9, 147.8, 149.5, 153.2, 153.7; FTIR: ν_{max} 2954 (w), 2836 (w), 1597 (m), 1505 (s), 1229 (s), 1125 (s), 1023 (m), 1005 (m), 979 (m); HRMS (ESI-TOF) *m/z* $[M+H]^+$ calculated for $C_{29}H_{35}N_2O_5Si$: 519.2310. Found: 519.2291.

1-(3,4,5-Trimethoxyphenyl)-5-(3-phenylmethoxy-4-methoxyphenyl)-pyrazole (4). Pyrazoles **3a** and **3b** (86 mg, 0.166 mmol, 95:5) and TBAF in THF (1.7 mL, 1.7 mmol) were subjected to general procedure E, affording pyrazole **4** as a yellow oil (50 mg, 67%). ^{1}H NMR (400 MHz, $CDCl_3$) δ 3.67 (6H, s), 3.84 (3H, s), 3.88 (3H, s), 4.97 (2H, s), 6.39 (1H, d, *J* = 2.0 Hz), 6.49 (2H, s), 6.77 (1H, s), 6.83-6.85 (2H, m), 7.26-7.34 (5H, m), 7.66 (1H, d, *J* =

2.0 Hz); ^{13}C NMR (101 MHz, $CDCl_3$) δ 56.1, 56.2, 61.1, 71.3, 102.9, 107.3, 111.6, 114.8, 122.2, 123.1, 127.1, 128.1, 128.7, 135.9, 136.8, 137.3, 140.1, 142.9, 148.0, 149.9, 153.2; FTIR: ν_{max} 2936 (w), 2836 (w), 1598 (m), 1508 (s), 1454 (m), 1415 (m), 1230 (s), 1118 (s), 1019 (m), 1002 (m); HRMS (ESI-TOF) *m/z* $[M+H]^+$ calculated for $C_{26}H_{27}BN_2O_5$: 447.1914. Found: 447.1925.

1-(3,4,5-Trimethoxyphenyl)-5-(3-hydroxy-4-methoxyphenyl)-pyrazole (5). Pyrazole **4** (139 mg, 0.311 mmol) and Pd/C (31 mg) were subjected to general procedure G, affording pyrazole **5** as a colourless solid (75 mg, 68%). M.p.: 102-103 °C; ^{1}H NMR (400 MHz, $CDCl_3$) δ 3.68 (6H, s), 3.83 (3H, s), 3.86 (3H, s), 5.99 (1H, br), 6.42 (1H, d, *J* = 2.0 Hz), 6.53 (2H, s), 6.69 (1H, dd, *J* = 8.5, 2.0 Hz), 6.76 (1H, d, *J* = 8.5, Hz), 6.87 (1H, d, *J* = 2.0, Hz), 7.65 (1H, d, *J* = 2.0 Hz); ^{13}C NMR (101 MHz, $CDCl_3$) δ 56.0, 56.2, 61.1, 102.9, 107.9, 110.6, 115.2, 121.0, 123.8, 135.9, 137.2, 140.1, 142.9, 145.6, 146.8, 153.1; FTIR: ν_{max} 3133 (br), 2933 (w), 2840 (w), 1601 (m), 1499 (s), 1458 (m), 1420 (m), 1272 (m), 1232 (s), 1118 (s), 1010 (m), 1002 (m), 933 (m); HRMS (ESI-TOF) *m/z* $[M+H]^+$ calculated for $C_{19}H_{21}N_2O_5$: 357.1445. Found: 357.1446; HPLC: Ret. Time: 13.65 min, Purity 96.3%.

N*-(3-Hydroxy-4-methoxyphenyl)sydnone (6).** 2-((3-Hydroxy-4-methoxyphenyl)amino) acetic acid (0.97 g, 4.9 mmol) was dissolved in 1,2-dimethoxethane (20 mL) and *iso*amylnitrite (0.58 g, 4.9 mmol) was added and the reaction stirred for 3 hours at room temperature. Volatiles were removed *in vacuo* at <30 ^{o}C and the crude material triturated with petroleum ether:diethyl ether (20:1). ***Caution nitrosamines are highly toxic and carcinogenic. The crude material was suspended in dichloromethane (20 mL) and cooled at 0 ^{o}C. Trifluoracetic anhydride (1.56 g, 7.41 mmol) was added and the reaction stirred for 1.5 hours at r.t. A small amount of water was added and the mixture basified with sodium bicarbonate and extracted with dichloromethane. The combined organic layers were dried over $MgSO_4$ and volatiles removed *in vacuo*. **6** was isolated as a brown solid (0.29 g, 28%).

The product could be further purified by recrystallization from ethanol. M.p.: 205-209 °C (dec.); ^{1}H NMR (400 MHz, DMSO-d_6): δ 3.87 (3H, s), 7.18 (1H, d, *J* = 9.0 Hz), 7.30 (1H, d, *J* = 2.5 Hz), 7.36 (1H, dd, *J* = 2.5, 9.0 Hz), 7.66 (1H, s), 9.99 (1H, s). ^{13}C NMR (101 MHz, DMSO-d_6): δ 56.0, 94.3, 108.1, 112.2, 112.5, 127.4, 147.4, 150.8, 168.5; FTIR: ν_{max} 3248 (br), 2924 (w), 1755 (s), 1720 (s), 1517 (s), 1285 (s), 1031 (m); HRMS calculated for $C_9H_9N_2O_4$ (ES^+)($+H^+$): 209.0562. Found: 209.0553.

4-(3,4,5-Trimethoxyphenyl)-*N*-(3-hydroxy-4-methoxyphenyl)sydnone. *N*-(3-Hydroxy-4-methoxyphenyl)sydnone (473 mg, 2.27 mmol) and 5-bromo-1,2,3-trimethoxybenzene (842 mg, 3.41 mmol) were subjected to general procedure A affording, 4-(3,4,5-trimethoxyphenyl)-*N*-(3-hydroxy-4-methoxyphenyl)sydnone as a colourless solid (402 mg, 47%). M.p.: 196-197 °C; ^{1}H NMR (400 MHz, $CDCl_3$) δ 3.67 (6H, s), 3.83 (3H, s), 4.00 (3H, s), 5.94 (1H, s), 6.59 (2H, s), 6.92-7.05 (2H, m), 7.09 (1H, s); ^{13}C NMR (101 MHz, $CDCl_3$) δ 56.1, 56.5, 61.0, 104.7, 108.0, 111.0, 111.7, 117.2, 119.9, 127.8, 138.5, 147.0, 149.5, 153.3, 167.2; FTIR: ν_{max} 3295 (br), 3082 (w), 2940 (w), 2836 (w), 1710 (s), 1600 (w), 1581 (m), 1509 (s), 1229 (s), 1125 (s) 1014 (m), 998 (m); HRMS calculated for $C_{18}H_{19}N_2O_7$ (ES^+)($+H^+$): 375.1192. Found: 375.1181.

4-(3,4,5-Trimethoxyphenyl)-*N*-(3-phenylmethoxy-4-methoxyphenyl)sydnone (7). A mixture of 4-(3,4,5-trimethoxyphenyl)-*N*-(3-hydroxy-4-methoxyphenyl)sydnone (402 mg, 1.07 mmol),benzyl bromide (368 mg, 2.15 mmol) and Hünigs base (278 mg, 2.15 mmol) were heated at 130 ^{o}C for 2 hours. The reaction was allowed to cool to ambient temperature and water was added. The mixture was extracted with dichloromethane and the combined organic layers washed with saturated ammonium chloride and brine, before drying over $MgSO_4$ and concentrating *in vacuo*. Flash silica chromatography (gradient starting with 100% 40-60 petroleum ether and ending with 40% ethyl acetate in 40-60 petroleum ether) afforded sydnone **7** as a yellow solid (296 mg, 60%). M.p.: 58-60 °C; ^{1}H NMR (400 MHz, $CDCl_3$) δ

3.62 (6H, s), 3.83 (3H, s), 3.96 (3H, s), 5.09 (2H, s), 6.51 (2H, s), 6.98-7.03 (2H, m), 7.09 (1H, dd, J = 8.5, 2.5 Hz), 7.29-7.36 (5H, m); ^{13}C NMR (101 MHz, $CDCl_3$) δ 56.1, 56.6, 61.1, 71.6, 104.5, 107.8, 110.6, 111.7, 118.3, 119.9, 127.3 (x2 C), 128.6, 128.9, 135.5, 138.5, 149.1, 152.5, 153.4, 167.1; FTIR: ν_{max} 2934 (w), 2836 (w), 1728 (s), 1581 (m), 1512 (s), 1226 (s), 1123 (s), 999 (s); HRMS (ESI-TOF) *m/z* $[M+H]^+$ calculated for $C_{25}H_{25}N_2O_7$: 465.1656. Found: 465.1668.

1-(3-Phenylmethoxy-4-methoxyphenyl)-3-(trimethylsilyl)-5-(3,4,5-trimethoxyphenyl)-pyrazole (8a, major) and 1-(3-phenylmethoxy-4-methoxyphenyl)-4-(trimethylsilyl)-5-(3,4,5-trimethoxyphenyl)-pyrazole (8b, minor). Sydnone **7** (290 mg, 0.624 mmol) and trimethylsilylacetylene (245 mg, 2.50 mmol) were subjected to general procedure B, affording an inseparable mixture of pyrazoles **8a** and **8b** as an orange oil (256 mg, 79%, 95:5). ^{1}H NMR (400 MHz, $CDCl_3$) δ 0.36 (9H, s), 3.65 (6H, s), 3.84 (3H, s), 3.87 (3H, s), 5.02 (2H, s), 6.38 (2H, s), 6.56 (1H, s), 6.83 (1H, d, J = 8.5 Hz), 6.88 (1H, dd, J = 8.5, 2.5 Hz), 6.95 (1H, d, J = 2.5 Hz), 7.27-7.34 (5H, m); ^{13}C NMR (101 MHz, $CDCl_3$) δ -0.9, 56.1, 56.4, 61.0, 71.3, 106.0, 111.5, 112.0, 113.3, 118.6, 126.3, 127.3, 128.1, 128.6, 133.6, 136.6, 137.8, 143.0, 148.3, 149.2, 153.1, 153.6; FTIR: ν_{max} 2951 (w), 2834 (w), 1584 (m), 1514 (s), 1236 (s), 1126 (s), 1005 (m), 978 (m); HRMS (ESI-TOF) *m/z* $[M+H]^+$ calculated for $C_{29}H_{35}N_2O_5Si$: 519.2310. Found: 519.2314.

1-(3-Phenylmethoxy-4-methoxyphenyl)-5-(3,4,5-trimethoxyphenyl)-pyrazole (9). Pyrazoles **8a** and **8b** (256 mg, 0.494 mmol, 95:5) and TBAF in THF (5 mL, 5 mmol) were subjected to general procedure E, affording pyrazole **9** as a yellow oil (137 mg, 62%). Product was contaminated with ~10% unknown by-product. ^{1}H NMR (400 MHz, $CDCl_3$) δ 3.64 (6H, s), 3.83 (3H, s), 3.86 (3H, s), 5.01 (2H, s), 6.38 (2H, s), 6.45 (1H, d, J = 2.0 Hz), 6.81-6.84 (2H, m), 6.93-6.97 (1H, m), 7.25-7.36 (5H, m), 7.65 (1H, d, J = 2.0 Hz); ^{13}C NMR (101 MHz, $CDCl_3$) δ 56.0, 56.3, 61.0, 71.2, 106.0, 107.0, 111.3, 111.6, 118.3, 125.9, 127.2,

127.3, 128.0, 128.6, 133.3, 136.5, 139.9, 142.9, 148.2, 149.1, 153.0; FTIR: ν_{max} 2934 (w), 2836 (w), 1584 (m), 1512 (s), 1414 (m), 1236 (s), 1121 (s), 1002 (m), 910 (m); HRMS (ESI-TOF) *m/z* $[M+H]^+$ calculated for $C_{26}H_{27}BN_2O_5$: 447.1914. Found: 447.1914.

1-(3-Hydroxy-4-methoxyphenyl)-5-(3,4,5-trimethoxyphenyl)-pyrazole (10). Pyrazole **9** (137 mg, 0.307 mmol) and Pd/C (31 mg) for 24 hours were subjected to general procedure G, affording pyrazole **10** as a colourless solid (76 mg, 69%). M.p.: 55-58 °C; ^{1}H NMR (400 MHz, $CDCl_3$) δ 3.68 (6H, s), 3.85 (3H, s), 3.88 (3H, s), 5.98 (1H, br), 6.43 (2H, s), 6.46 (1H, d, *J* = 2.0 Hz), 6.75 (1H, dd, *J* = 8.5, 2.5 Hz), 6.78 (1H, d, *J* = 8.5, Hz), 6.97 (1H, d, *J* = 2.5, Hz), 7.66 (1H, d, *J* = 2.0 Hz); ^{13}C NMR (101 MHz, $CDCl_3$) δ 56.1, 56.3, 61.1, 106.1, 107.0, 110.4, 112.7, 117.5, 126.0, 133.9, 138.0, 139.9, 143.1, 145.9, 146.3, 153.1; FTIR: ν_{max} 3146 (br), 2941 (w), 2836 (w), 1585 (m), 1511 (s), 1498 (s), 1416 (m), 1239 (s), 1120 (s), 1000 (m); HRMS (ESI-TOF) *m/z* $[M+H]^+$ calculated for $C_{19}H_{21}N_2O_5$: 357.1445. Found: 357.1444; HPLC: Ret. Time: 13.54 min, Purity 95.2%.

4-(3,4,5-Trimethoxyphenyl)-*N*-methylsydnone (11). *N*-Methylsydnone (250 mg, 2.50 mmol) and 5-bromo-1,2,3-trimethoxybenzene (926 mg, 3.75 mmol) were subjected to general procedure A, affording **11** as a colourless solid (571 mg, 86%). M.p.: 123-124 °C; ^{1}H NMR (400 MHz, $CDCl_3$) δ 3.86 (3H, s), 3.87 (6H, s), 4.12 (3H, s), 6.74 (2H, s); ^{13}C NMR (101 MHz, $CDCl_3$) δ 39.0, 56.5, 61.1, 105.7, 108.2, 119.6, 139.2, 153.9, 167.3; FTIR: ν_{max} 2932 (w), 2858 (w), 1726 (s), 1585 (m), 1241 (m), 1225 (m), 1124 (s), 998 (m); HRMS (ESI-TOF) *m/z* $[M+H]^+$ calculated for $C_{12}H_{15}N_2O_5$: 267.0981. Found: 267.0970.

4-(3,4,5-Trimethoxyphenyl)-*N*-benzylsydnone (12). *N*-Benzylsydnone (500 mg, 2.84 mmol) and 5-bromo-1,2,3-trimethoxybenzene (1.05 g, 4.26 mmol) were subjected to general procedure A, affording **12** as a colourless solid (570 mg, 59%). M.p.: 101 °C; ^{1}H NMR (400 MHz, $CDCl_3$) δ 3.69 (6H, s), 3.84 (3H, s), 5.52 (2H, s), 6.52 (2H, s), 7.18-7.24 (2H, m), 7.37-

7.43 (3H, m); ^{13}C NMR (101 MHz, $CDCl_3$) δ 55.5, 56.2, 61.0, 106.1, 108.6, 119.4, 127.1, 129.5, 129.5, 132.0, 139.2, 153.8, 167.6; FTIR: ν_{max} 2829 (w), 1727 (s), 1712 (s), 1578 (m), 1521 (m), 1223 (s), 1131 (s), 1000 (s); HRMS (ESI-TOF) *m/z* $[M+H]^+$ calculated for $C_{18}H_{19}N_2O_5$: 343.1294. Found: 343.1278.

4-(3-Phenylmethoxy-4-methoxyphenyl)-*N*-methylsydnone (13). *N*-Methylsydnone (500 mg, 5.00 mmol) and 1-bromo-3-phenylmethoxy-4-methoxybenzene (2.2 g, 7.5 mmol) were subjected to general procedure A affording **13** as a tan solid (1.105 g, 71%). M.p.: 99 °C; ^{1}H NMR (400 MHz, $CDCl_3$) δ 3.83 (3H, s), 3.92 (3H, s), 5.19 (2H, s), 6.96 (1H, d, *J* = 8.5 Hz), 7.04 (1H, d, *J* = 2.0 Hz), 7.10 (1H, dd, *J* = 8.5, 2.0 Hz), 7.27-7.33 (1H, m), 7.34-7.40 (2H, m), 7.41-7.47 (2H, m); ^{13}C NMR (101 MHz, $CDCl_3$) δ 38.6, 56.2, 71.2, 108.1, 112.2, 113.8, 116.7, 121.4, 127.4, 128.1, 128.8, 136.8, 148.3, 150.6, 167.4; FTIR: ν_{max} 2970 (w), 1723 (s), 1532 (m), 1450 (m), 1380 (m), 1305 (m), 1230 (m), 1225 (m), 1150 (s), 990 (s); HRMS (ESI-TOF) *m/z* $[M+H]^+$ calculated for $C_{17}H_{17}N_2O_4$: 313.1188. Found: 313.1185.

4-(3-Phenylmethoxy-4-methoxyphenyl)-*N*-benzylsydnone (14). *N*-Benzylsydnone (1.00 g, 5.68 mmol) and 1-bromo-3-phenylmethoxy-4-methoxybenzene (2.50 g, 8.51 mmol) were subjected to general procedure A, affording **14** as a tan solid (1.21 g, 55%). M.p.: 144-145 °C; ^{1}H NMR (400 MHz, $CDCl_3$) δ 3.90 (3H, s), 5.01 (2H, s), 5.34 (2H, s), 6.87 (1H, d, *J* = 2.0 Hz), 6.91 (1H, d, *J* = 8.5 Hz), 6.96 (1H, dd, *J* = 8.5, 2.0 Hz), 7.06-7.11 (2H, m), 7.27-7.40 (8H, m); ^{13}C NMR (101 MHz, $CDCl_3$) δ 55.2, 56.2, 71.0, 108.0, 112.2, 114.1, 116.5, 122.4, 127.5, 127.6, 128.2, 128.8, 129.4, 129.5, 131.7, 136.6, 148.4, 150.8, 167.7; FTIR: ν_{max} 3008 (w), 2836 (w), 1720 (s), 1703 (m), 1260 (m), 1226 (m), 1176 (m), 1023 (s); HRMS (ESI-TOF) *m/z* $[M+H]^+$ calculated for $C_{23}H_{21}N_2O_4$: 389.1501. Found: 389.1519.

1-(Methyl)-3-(trimethylsilyl)-4-(pinacolatoborolane)-5-(3,4,5-trimethoxyphenyl)-pyrazole (15a, major) and 1-(4-methyl)-3-(trimethylsilyl)-5-(3,4,5-trimethoxyphenyl)-

pyrazole (15b, minor). Sydnone **11** (200 mg, 0.751 mmol) and 4,4,5,5-tetramethyl-2-[2-(trimethylsilyl)ethynyl]-1,3,2-dioxaborolane (337 mg, 1.50 mmol) were subjected to general procedure C, affording an inseparable mixture of pyrazoles **15a** and **15b** as a yellow oil (309 mg, 92% 5:1). ^{1}H NMR (400 MHz, $CDCl_3$) δ 0.36 (9H, s), 1.18 (12H, s), 3.80 (3H, s), 3.85 (6H, s), 3.90 (3H, s), 6.59 (2H, s); ^{13}C NMR (101 MHz, $CDCl_3$) δ -0.4, 25.0, 37.2, 56.2, 61.1, 83.0, 107.8, 126.9, 138.1, 150.8, 152.6, 158.8; FTIR: ν_{max} 2976 (m), 1585 (m), 1497 (s), 1411 (s), 1240 (s), 1128 (s), 1048 (m); HRMS (ESI-TOF) *m/z* $[M+H]^+$ calculated for $C_{22}H_{36}N_2O_5Si$: 447.2481. Found: 447.2488.

1-(Benzyl)-3-(trimethylsilyl)-4-(pinacolatoborolane)-5-(3,4,5-trimethoxyphenyl)-pyrazole (16a, major) and 1-(benzyl)-3-(trimethylsilyl)-5-(3,4,5-trimethoxyphenyl)-pyrazole (16b, minor). Sydnone **12** (200 mg, 0.584 mmol) and 4,4,5,5-tetramethyl-2-[2-(trimethylsilyl)ethynyl]-1,3,2-dioxaborolane (262 mg, 1.17 mmol) were subjected to general procedure C, affording an inseparable mixture of pyrazoles **16a** and **16b** was isolated as a yellow oil (202 mg, 66%, 9:1). ^{1}H NMR (400 MHz, $CDCl_3$) δ 0.37 (9H, s), 1.19 (12H, s), 3.63 (6H, s), 3.87 (3H, s), 5.28 (2H, s), 6.40 (2H, s) 7.05 (2H, d, J = 7.0 Hz), 7.17-7.29 (3H, m); ^{13}C NMR (101 MHz, $CDCl_3$) δ -0.3, 25.0, 53.1, 55.9, 61.0, 83.0, 107.7, 112.8, 127.0, 127.3, 128.5, 138.0, 138.5, 150.9, 152.4, 158.8; FTIR: ν_{max} 2976 (w), 1585 (m), 1496 (m), 1236 (s), 1124 (s), 1038 (s); HRMS (ESI-TOF) *m/z* $[M+H]^+$ calculated for $C_{28}H_{40}{}^{11}BN_2O_5Si$: 523.2794. Found: 523.2801.

1-(Methyl)-3-(trimethylsilyl)-4-(pinacolatoborolane)-5-(3-phenylmethoxy-4-methoxyphenyl)-pyrazole (17a, major) and 1-(methyl)-3-(trimethylsilyl)-5-(3-phenylmethoxy-4-methoxyphenyl)-pyrazole (17b, minor). Sydnone **13** (200 mg, 0.640 mmol) and 4,4,5,5-tetramethyl-2-[2-(trimethylsilyl)ethynyl]-1,3,2-dioxaborolane (287 mg, 1.28 mmol) were subjected to general procedure C, affording an inseparable mixture of pyrazoles **17a** and **17b** as a yellow oil (230 mg, 73%, 4:1). ^{1}H NMR (400 MHz, $CDCl_3$) δ

0.37 (9H, s), 1.20 (12H, s), 3.57 (3H, s), 3.94 (3H, s), 5.18 (2H, s), 6.91-6.94 (3H, m) 7.28-7.32 (1H, m), 7.33-7.39 (2H, m), 7.41-7.46 (2H, m); ^{13}C NMR (101 MHz, $CDCl_3$) δ -0.4, 25.0, 36.9, 56.1, 71.0, 82.9, 110.9, 116.5, 122.0, 123.6, 127.3, 128.0, 128.7, 137.1, 147.1, 149.7, 150.7, 158.7; FTIR: ν_{max} 2977 (w), 1498 (m), 1311 (s), 1250 (s), 1139 (s), 1046 (m), 1026 (m); HRMS (ESI-TOF) *m/z* $[M+H]^+$ calculated for $C_{27}H_{38}{}^{11}BN_2O_4Si$: 493.2694. Found: 493.2718.

1-(Benzyl)-3-(trimethylsilyl)-4-(pinacolatoborolane)-5-(3-phenylmethoxy-4-methoxyphenyl)-pyrazole (18a, major) and 1-(benzyl)-3-(trimethylsilyl)-5-(3-phenylmethoxy-4-methoxyphenyl)-pyrazole (18b, minor). Sydnone **14** (200 mg, 0.515 mmol) and 4,4,5,5-tetramethyl-2-[2-(trimethylsilyl)ethynyl]-1,3,2-dioxaborolane (231 mg, 1.03 mmol) were subjected to general procedure C, affording an inseparable mixture of pyrazoles **18a** and **18b** as a yellow oil (187 mg, 64%, 9:1). ^{1}H NMR (400 MHz, $CDCl_3$) δ 0.39 (9H, s), 1.19 (12H, s), 3.91 (3H, s), 4.90 (2H, s), 5.16 (2H, s), 6.78-6.82 (2H, m), 6.84 (1H, d, *J* = 8.0 Hz), 6.92-6.98 (2H, m), 7.18-7.24 (2H, m), 7.27-7.41 (6H, m); ^{13}C NMR (101 MHz, $CDCl_3$) δ -0.3, 25.0, 52.9, 56.1, 70.7, 83.0, 110.9, 115.9, 123.6, 123.9, 127.1, 127.2, 127.4, 128.0, 128.4, 128.7, 137.1, 138.3, 147.2, 149.7, 150.8, 158.7; FTIR: ν_{max} 2977 (w), 1497 (m), 1452 (m), 1250 (s), 1141 (s), 1029 (m) 908 (s); HRMS (ESI-TOF) *m/z* $[M+H]^+$ calculated for $C_{33}H_{42}{}^{11}BN_2O_4Si$: 569.3007. Found: 569.3010.

1-(Methyl)-3-(trimethylsilyl)-4-(3-phenylmethoxy-4-methoxyphenyl)-5-(3,4,5-trimethoxyphenyl)-pyrazole (19, major) and 1-(methyl)-3-(trimethylsilyl)-5-(3,4,5-trimethoxyphenyl)-pyrazole (15b, minor). Pyrazoles **15a** and **15b** (498 mg, 1.12 mmol) and 1-bromo-3-phenylmethoxy-4-methoxybenzene (491 mg, 1.67 mmol) were subjected to general procedure D, affording an inseparable mixture of pyrazoles **19** and **15b** as a yellow oil (409 mg, 69%, 3:1). ^{1}H NMR (400 MHz, $CDCl_3$) δ 0.14 (9H, s), 3.68 (6H, s), 3.84 (3H, s), 3.87 (3H, s), 3.88 (3H, s), 5.00 (2H, s), 6.34 (2H, s) 6.68 (1H, d, *J* = 2.0 Hz), 6.71 (1H, d, *J* =

8.0, 2.0 Hz), 6.79 (1H, d, *J* = 8.0 Hz), 7.25-7.35 (5H, m); ^{13}C NMR (101 MHz, $CDCl_3$) δ -0.2, 37.7, 56.1, 56.2, 61.0, 71.1, 106.3, 107.3, 111.3, 112.6, 116.8, 123.8, 125.7, 127.1, 127.7, 127.9, 128.6, 137.2, 141.3, 147.5, 148.6, 150.5, 153.1; FTIR: ν_{max} 2957 (w), 2934 (w), 1580 (m), 1237 (s), 1127 (s), 1008 (m); HRMS (ESI-TOF) *m/z* $[M+H]^+$ calculated for $C_{30}H_{37}N_2O_5Si$: 533.2472. Found: 533.2469.

1-(Benzyl)-3-(trimethylsilyl)-4-(3-phenylmethoxy-4-methoxyphenyl)-5-(3,4,5-trimethoxyphenyl)-pyrazole (20, major) and 1-(benzyl)-3-(trimethylsilyl)-5-(3,4,5-trimethoxyphenyl)-pyrazole (16b, minor). Pyrazoles **16a** and **16b** (307 mg, 0.587 mmol) and 1-bromo-3-phenylmethoxy-4-methoxybenzene (258 mg, 0.881 mmol) were subjected to general procedure D, affording an inseparable mixture of pyrazoles **20** and **16b** as a yellow oil (257 mg, 72%, 9:1). ^{1}H NMR (400 MHz, $CDCl_3$) δ 0.20 (9H, s), 3.48 (6H, s), 3.82 (3H, s), 3.86(3H, s), 4.99 (2H, s), 5.33 (2H, s), 6.18 (2H, s) 6.72-6.77 (2H, m), 6.80 (1H, d, *J* = 8.0 Hz), 7.12-7.17 (2H, m), 7.22-7.38 (8H, m); ^{13}C NMR (101 MHz, $CDCl_3$) δ -0.2, 53.6, 55.8, 56.0, 60.9, 71.1, 106.1, 107.3, 111.2, 116.6, 123.6, 125.7, 126.4, 127.0, 127.1, 127.4, 127.8, 128.5, 128.6, 137.1, 137.7, 138.5, 141.0, 147.4, 148.5, 150.7, 152.8; FTIR: ν_{max} 2956 (w), 2835 (w), 1583 (m), 1495 (m), 1244 (s), 1125 (s), 1026 (m), 1004 (m), 907 (m); HRMS (ESI-TOF) *m/z* $[M+H]^+$ calculated for $C_{36}H_{41}N_2O_5Si$: 609.2779. Found: 609.2772.

1-(Methyl)-3-(trimethylsilyl)-4-(3,4,5-trimethoxyphenyl)-5-(3-phenylmethoxy-4-methoxyphenyl)-pyrazole (21, major) and 1-(methyl)-3-(trimethylsilyl)-5-(3-phenylmethoxy-4-methoxyphenyl)-pyrazole (17b, minor). Pyrazoles **17a** and **17b** (215 mg, 0.437 mmol) and 5-bromo-1,2,3-trimethoxybenzene (218 mg, 0.883 mmol) were subjected to general procedure D, affording an inseparable mixture of pyrazoles **21** and **17b** was isolated as a yellow oil (137 mg, 60%, 4:1). ^{1}H NMR (400 MHz, $CDCl_3$) δ 0.21 (9H, s), 3.68 (9H, s), 3.83 (3H, s), 3.87 (3H, s), 5.01 (2H, s), 6.32 (2H, s) 6.68 (1H, d, *J* = 2.0 Hz), 6.77 (1H, d, *J* = 8.5, 2.0 Hz), 6.85 (1H, d, *J* = 8.5 Hz), 7.25-7.38 (5H, m); ^{13}C NMR (101

MHz, $CDCl_3$) δ -0.2, 37.3, 56.0, 56.3, 61.0, 71.0, 104.7, 107.7, 111.5, 116.0, 122.6, 123.2, 127.0, 127.9, 128.6, 130.7, 136.8, 140.8, 147.6, 149.6, 149.8, 152.5, 153.4; FTIR: ν_{max} 2934 (w), 1580 (m), 1493 (m), 1233 (s), 1125 (s), 1006 (m); HRMS (ESI-TOF) *m/z* $[M+H]^+$ calculated for $C_{30}H_{37}N_2O_5Si$: 533.2472. Found: 533.2497.

1-(Benzyl)-3-(trimethylsilyl)-4-(3,4,5-trimethoxyphenyl)-5-(3-phenylmethoxy-4-methoxyphenyl)-pyrazole (22) and 1-(benzyl)-3-(trimethylsilyl)-5-(3-phenylmethoxy-4-methoxyphenyl)-pyrazole (18b). Pyrazoles **18a** and **18b** (162 mg, 0.285 mmol) and 5-bromo-1,2,3-trimethoxybenzene (136 mg, 0.550 mmol) were subjected to general procedure D, affording an inseparable mixture of pyrazoles **22** and **18b** as a yellow oil (85 mg, 49%, 3:1). ^{1}H NMR (400 MHz, $CDCl_3$) δ 0.24 (9H, s), 3.66 (6H, s), 3.82 (3H, s), 3.86 (3H, s), 4.78 (2H, s), 5.22 (2H, s), 6.31 (2H, s) 6.56 (1H, d, *J* = 2.0 Hz), 6.62 (1H, d, *J* = 8.5, 2.0 Hz), 6.77 (1H, d, *J* = 8.5 Hz), 7.08 (2H, dd, *J* = 9.0, 7.0 Hz), 7.22-7.35 (8H, m); ^{13}C NMR (101 MHz, $CDCl_3$) δ -0.1, 53.5, 56.1, 56.4, 61.1, 70.7, 107.7, 109.1, 111.5, 115.8, 122.1, 126.7, 127.2 (x2 C), 127.5, 128.0, 128.6 (x2 C), 130.6, 136.8, 138.2, 140.9, 147.7, 149.7, 150.3, 152.5, 154.0; FTIR: ν_{max} 2955 (w), 2934 (w), 2834 (w), 1581 (m), 1494 (m), 1232 (s), 1124 (s), 1006 (m); HRMS (ESI-TOF) *m/z* $[M+H]^+$ calculated for $C_{36}H_{41}N_2O_5Si$: 609.2784. Found: 609.2785.

1-(Methyl)-4-(3-phenylmethoxy-4-methoxyphenyl)-5-(3,4,5-trimethoxyphenyl)-pyrazole (23a) and 1-(methyl)-5-(3,4,5-trimethoxyphenyl)-pyrazole (23b). Pyrazoles **19** and **15b** (211 mg, 0.396 mmol, 3:1) and TBAF in THF (4 mL, 4 mmol) were subjected to general procedure E, affording a mixture of pyrazole **23a** and **23b** as a yellow oil (101 mg, 55%, 95:5). ^{1}H NMR (400 MHz, $CDCl_3$) δ 3.76 (6H, s), 3.83 (3H, s), 3.87 (3H, s), 3.89 (3H, s), 4.89 (2H, s), 6.48 (2H, s), 6.71 (1H, d, *J* = 2.0 Hz), 6.75-6.85 (2H, m), 7.20-7.32 (5H, m), 7.63 (1H, s); ^{13}C NMR (101 MHz, $CDCl_3$) δ 37.4, 56.1, 56.4, 61.1, 70.9, 106.4, 107.4, 112.0, 113.3, 120.0, 120.6, 125.8, 126.1, 127.1, 127.9, 128.6, 137.1, 137.2, 138.5, 139.4, 148.0,

148.2; FTIR: ν_{max} 2935 (w), 2835 (w), 1583 (m), 1409 (m), 1236 (s), 1123 (s), 1002 (m); HRMS (ESI-TOF) *m/z* $[M+H]^+$ calculated for $C_{27}H_{29}N_2O_5$: 461.2076. Found: 461.2090.

1-(Benzyl)-4-(3-phenylmethoxy-4-methoxyphenyl)-5-(3,4,5-trimethoxyphenyl)-pyrazole (24). Pyrazoles **20** and **16b** (244 mg, 0.401 mmol, 9:1) and TBAF in THF (4 mL, 4 mmol) were subjected to general procedure E, affording pyrazole **24** as a yellow oil (137 mg, 64%). ^{1}H NMR (400 MHz, $CDCl_3$) δ 3.59 (6H, s), 3.84 (3H, s), 3.87 (3H, s), 4.89 (2H, s), 5.22 (2H, s), 6.33 (2H, s), 6.76 (1H, d, *J* = 2.0 Hz), 6.79 (1H, d, *J* = 8.5 Hz), 6.85 (1H, dd, *J* = 8.5, 2.0 Hz), 7.04-7.08 (2H, m), 7.23-7.32 (8H, m), 7.74 (1H, s); ^{13}C NMR (101 MHz, $CDCl_3$) δ 53.6, 56.1 (x2 C), 61.1, 70.8, 107.5, 112.0, 113.1, 119.8, 120.8, 125.6, 125.8, 127.0, 127.1, 127.6, 127.8, 128.5, 128.6, 137.1, 137.6, 138.0, 138.4, 139.4, 148.0, 148.2, 153.5; FTIR: ν_{max} 2999 (w), 2934 (w), 2836 (w), 1580 (m), 1517 (m), 1451 (m), 1220 (s), 1136 (s), 1106 (m), 1024 (m), 1001 (m); HRMS (ESI-TOF) *m/z* $[M+H]^+$ calculated for $C_{33}H_{33}N_2O_5$: 537.2384. Found: 537.2386.

1-(Methyl)-4-(3,4,5-trimethoxyphenyl)-5-(3-phenylmethoxy-4-methoxyphenyl)-pyrazole (25). Pyrazoles **21** and **17b** (137 mg, 0.257 mmol, 4:1) and TBAF in THF (2.6 mL, 2.6 mmol) were subjected to general procedure E, affording pyrazole **25** as an orange oil (66 mg, 56%). ^{1}H NMR (400 MHz, $CDCl_3$) δ 3.59 (3H, s), 3.62 (6H, s), 3.80 (3H, s), 3.93 (3H, s), 5.11 (2H, s), 6.36 (2H, s), 6.80 (1H, d, *J* = 2.0 Hz), 6.87 (1H, dd, *J* = 8.0, 2.0 Hz), 6.96 (1H, d, *J* = 8.0 Hz), 7.24-7.38 (5H, m), 7.62 (1H, s); ^{13}C NMR (101 MHz, $CDCl_3$) δ 37.1, 55.9, 56.2, 61.0, 71.2, 104.3, 112.0, 116.2, 120.8, 122.7, 123.6, 127.2, 128.1, 128.7 (x2 C), 136.4, 136.6, 137.0, 139.7, 148.1, 150.3, 153.1; FTIR: ν_{max} 3002 (w), 2934 (w), 1584 (m), 1521 (m), 1418 (m), 1373 (m), 1253 (s), 1124 (s), 1021 (m), 1007 (m); HRMS (ESI-TOF) *m/z* $[M+H]^+$ calculated for $C_{27}H_{29}N_2O_5$: 461.2071. Found: 461.2070.

1-(Benzyl)-4-(3,4,5-trimethoxyphenyl)-5-(3-phenylmethoxy-4-methoxyphenyl)-pyrazole (26). Pyrazoles **22** and **18b** (158 mg, 0.260 mmol, 4:1) and TBAF in THF (2.6 mL, 2.6 mmol) were subjected to general procedure E, affording pyrazole **26** as an orange oil (103 mg, 74%). ^{1}H NMR (400 MHz, $CDCl_3$) δ 3.61 (6H, s), 3.80 (3H, s), 3.91 (3H, s), 4.88 (2H, s), 5.13 (2H, s), 6.37 (2H, s), 6.67 (1H, d, *J* = 2.0 Hz), 6.79 (1H, dd, *J* = 8.0, 2.0 Hz), 6.90 (1H, d, *J* = 8.0 Hz), 6.98-7.03 (2H, m), 6.24-7.33 (8H, m), 7.79 (1H, s); ^{13}C NMR (101 MHz, $CDCl_3$) δ 53.3, 55.9, 56.2, 61.0, 70.8, 104.3, 111.9, 116.0, 121.2, 122.5, 123.8, 127.1, 127.3, 127.7, 128.1, 128.6, 128.7 (x2 C), 136.5, 136.6, 137.6, 137.7, 140.0, 148.1, 150.3, 153.2; FTIR: ν_{max} 2935 (w), 2835 (w), 1583 (m), 1520 (m), 1454 (m), 1373 (m), 1245 (s), 1123 (s), 1002 (s); HRMS (ESI-TOF) *m/z* $[M+H]^+$ calculated for $C_{33}H_{33}N_2O_5$: 537.2384. Found: 537.2383.

1-(Methyl)-4-(3-hydroxy-4-methoxyphenyl)-5-(3,4,5-trimethoxyphenyl)-pyrazole (27). Pyrazoles **23a** and **23b** (100 mg, 0.217 mmol) and Pd/C (22 mg) were subjected to general procedure G, affording pyrazole **27** was isolated as a colourless solid (47 mg, 58%). M.p.: 210 °C; ^{1}H NMR (400 MHz, $CDCl_3$) δ 3.77 (3H, s), 3.79 (6H, s), 3.85 (3H, s), 3.92 (3H, s), 5.57 (1H, s), 6.50 (2H, s), 6.66 (1H, dd, *J* = 8.5, 2.0 Hz), 6.72 (1H, d, *J* = 8.5 Hz), 6.85 (1H, d, *J* = 2.0 Hz), 7.67 (1H, s); ^{13}C NMR (101 MHz, $CDCl_3$) δ 37.4, 56.0, 56.3, 61.1, 107.4, 110.8, 113.8, 119.1, 120.6, 125.9, 126.5, 137.4, 138.4, 139.5, 145.3, 145.6, 153.6; FTIR: ν_{max} 3347 (br), 1582 (m), 1458 (m), 1406 (m), 1270 (m), 1232 (s), 1129 (s), 1028 (m), 997 (m); HRMS (ESI-TOF) *m/z* $[M+H]^+$ calculated for $C_{20}H_{23}N_2O_5$: 371.1607. Found: 371.1611; HPLC: Ret. Time: 11.31 min, Purity 98.5%.

4-(3-Hydroxy-4-methoxyphenyl)-5-(3,4,5-trimethoxyphenyl)-pyrazole (28) and 1-(benzyl)-4-(3-hydroxy-4-methoxyphenyl)-5-(3,4,5-trimethoxyphenyl)-pyrazole (29). Pyrazole **24** (126 mg, 0.235 mmol) and Pd/C (24 mg) were subjected to general procedure G, affording pyrazole **28** as a colourless solid (25 mg, 30%) and pyrazole **29** as a colourless

solid (23 mg, 22%). **28**: M.p.: 198-200 °C; ^{1}H NMR (400 MHz, $CDCl_3$) δ 3.73 (6H, s), 3.87 (3H, s), 3.90 (3H, s), 6.71 (2H, s), 6.81 (2H, app. d, *J* = 1.0 Hz), 6.96 (1H, app. t, *J* = 1.0 Hz), 7.65 (1H, s); ^{13}C NMR (101 MHz, $CDCl_3$) δ 56.2 (x2 C), 61.1, 105.4, 105.6, 110.8, 115.2, 119.8, 120.7, 126.5, 127.1, 129.9, 138.1, 145.7, 145.8, 153.4; FTIR: ν_{max} 3251 (m), 2966 (w), 2937 (w), 1587 (m), 1412 (m), 1274 (m), 1234 (s), 1121 (s), 1028 (m), 994 (m); HRMS (ESI-TOF) *m/z* $[M+H]^+$ calculated for $C_{19}H_{20}N_2O_5$: 357.1445. Found: 357.1443; HPLC: Ret. Time: 11.76 min, Purity 98.2%. **29**: M.p.: 126 °C; ^{1}H NMR (400 MHz, $CDCl_3$) δ 3.60 (6H, s), 3.84 (3H, s), 3.89 (3H, s), 5.22 (2H, s), 5.56 (1H, s), 6.33 (2H, s), 6.65-6.74 (2H, m), 6.87 (1H, d, *J* = 1.5 Hz), 7.06 (1H, d, *J* = 7.0 Hz), 7.19-7.33 (4H, m), 7.77 (1H, s); ^{13}C NMR (101 MHz, $CDCl_3$) δ 53.6, 56.1 (x2 C), 61.1, 107.6, 110.8, 113.6, 119.0, 120.8, 125.7, 126.5, 127.0, 127.6, 128.7, 138.0, 138.1, 138.5, 139.7, 145.3, 145.6, 153.4; FTIR: ν_{max} 3423 (m), 2926 (m), 2835 (w), 1579 (m), 1500 (m), 1231 (m), 1216 (m), 1124 (s), 1028 (m), 1000 (m); HRMS (ESI-TOF) *m/z* $[M+H]^+$ calculated for $C_{26}H_{26}N_2O_5$: 447.1914. Found: 447.1922; HPLC: Ret. Time: 16.32 min, Purity 95.7%.

4-(3-Hydroxy-4-methoxyphenyl)-5-(3,4,5-trimethoxyphenyl)-pyrazole (28). Pyrazole **38** (79 mg, 0.18 mmol) and Pd/C (18 mg) were subjected to general procedure G, affording pyrazole **28** as a colourless solid (18 mg, 29%). See above for characterization.

1-(Methyl)-4-(3,4,5-trimethoxyphenyl)-5-(3-hydroxy-4-methoxyphenyl)-pyrazole (30). Pyrazole **25** (177 mg, 0.384 mmol) and Pd/C (38 mg) were subjected to general procedure G, affording pyrazole **30** as a colourless solid (96 mg, 67%). M.p.: 149-150 °C; ^{1}H NMR (400 MHz, $CDCl_3$) δ 3.64 (6H, s), 3.74 (3H, s), 3.79 (3H, s), 3.92 (3H, s), 6.38 (1H, br), 6.41 (2H, s), 6.79 (1H, dd, *J* = 8.0, 2.0 Hz), 6.89-6.95 (2H, m), 7.68 (1H, s); ^{13}C NMR (101 MHz, $CDCl_3$) δ 37.2, 55.9, 56.1, 61.0, 104.4, 111.0, 116.5, 120.8, 122.4, 123.4, 128.8, 136.3, 137.0, 139.8, 146.1, 147.3, 153.1; FTIR: ν_{max} 3269 (br), 2940 (w), 1583 (m), 1373 (m), 1272 (m),

1227 (m), 1173 (m), 1123 (s), 1007 (m); HRMS (ESI-TOF) *m/z* $[M+H]^+$ calculated for $C_{20}H_{23}N_2O_5$: 371.1607. Found: 371.1605; HPLC: Ret. Time: 13.06 min, Purity 94.4%.

4-(3,4,5-Trimethoxyphenyl)-5-(3-hydroxy-4-methoxyphenyl)-pyrazole (31) and 1-(benzyl)-4-(3,4,5-trimethoxyphenyl)-5-(3-hydroxy-4-methoxyphenyl)-pyrazole (32). Pyrazole **26** (66 mg, 0.123 mmol) and Pd/C (15 mg) were subjected to general procedure G, affording pyrazole **31** as a colourless solid (12 mg, 27%) and pyrazole **32** as a tan solid (15 mg, 27%). **31**: M.p.: 90-93 °C; ^{1}H NMR (400 MHz, $CDCl_3$) δ 3.73 (6H, s), 3.86 (3H, s), 3.88 (3H, s), 6.51 (2H, s), 6.80 (1H, d, *J* = 8.5 Hz), 6.94 (1H, dd, *J* = 8.5, 2.0 Hz), 7.13 (1H, d, *J* = 2.0 Hz), 7.67 (1H, s); ^{13}C NMR (101 MHz, $CDCl_3$) δ 56.1, 56.2, 61.1, 105.7, 110.9, 114.7, 119.6, 120.6, 124.2, 128.8, 135.9, 136.9, 142.6, 145.8, 147.1, 153.3; FTIR: ν_{max} 3282 (br), 2934 (w), 2838 (w), 1584 (m), 1449 (m), 1411 (m), 1251 (m), 1231 (m), 1122 (s), 1019 (m); HRMS (ESI-TOF) *m/z* $[M+H]^+$ calculated for $C_{19}H_{20}N_2O_5$: 357.1445. Found: 357.1440; HPLC: Ret. Time: 12.08 min, Purity 95.1%. **32**: M.p.: 167-168 °C; ^{1}H NMR (400 MHz, $CDCl_3$) δ 3.65 (6H, s), 3.80 (3H, s), 3.93 (3H, s), 5.22 (2H, s), 5.66 (1H, s), 6.43 (2H, s), 6.72 (1H, dd, *J* = 8.0, 2.0 Hz), 6.83-6.88 (2H, m), 7.03-7.08 (2H, m), 7.23-7.29 (3H, m), 7.78 (1H, s); ^{13}C NMR (101 MHz, $CDCl_3$) δ 56.1, 56.2, 56.3, 61.1, 105.9, 110.5, 115.0, 120.7, 121.0, 127.0, 128.1, 128.3, 129.0, 129.1, 136.5, 136.9, 145.5, 146.4, 148.5, 153.2 (one sp^2 carbon not observed); FTIR: ν_{max} 2929 (br), 1584 (m), 1520 (m), 1374 (m), 1246 (m), 1120 (s), 1007 (m); HRMS (ESI-TOF) *m/z* $[M+H]^+$ calculated for $C_{26}H_{26}N_2O_5$: 447.1914. Found: 447.1914; HPLC: Ret. Time: 16.07 min, Purity 98.6%.

4-(3,4,5-Trimethoxyphenyl)-5-(3-hydroxy-4-methoxyphenyl)-pyrazole (31). A solution of pyrazole **40** (274 mg, 0.614 mmol) in methanol (6 mL) and AcOH (6 drops) was flowed through a H-Cube continuous flow hydrogenator (1 mL min^{-1}) with a 10% Pd/C catalyst cartridge at 80 °C using controlled H_2 mode (80 bar) as a continuous loop. Once the reaction was complete by TLC analysis, the system was washed with methanol (10 mL). The reaction

was subsequently neutralized with $NaHCO_3$ then filtered and the volatiles were removed *in vacuo*. Flash silica chromatography (gradient starting with 100% 40-60 petroleum ether and ending with 100% ethyl acetate in 40-60 petroleum ether) afforded pyrazole **31** as a colourless solid (144 mg, 66%). See above for characterization.

1-(Methyl)-3-(3,4,5-trimethoxyphenyl)-pyrazole (33). *N*-Methylsydnone (150 mg, 1.50 mmol) and 3,4,5-trimethoxyphenylacetylene (576 mg, 3.00 mmol) were subjected to general procedure B, affording pyrazole **33** as an orange oil (236 mg, 63%, >98:2). ^{1}H NMR (400 MHz, $CDCl_3$) δ 3.83 (3H, s), 3.89 (9H, s), 6.45 (1H, d, J = 2.0 Hz), 6.99 (2H, s), 7.33 (1H, d, J = 2.0 Hz); ^{13}C NMR (101 MHz, $CDCl_3$) δ 39.0, 56.1, 60.9, 102.6, 102.7, 129.4, 131.5, 137.6, 151.4, 153.4; FTIR: ν_{max} 2930 (w), 2827 (w), 1588 (m), 1507 (m), 1401 (m), 1232 (s), 1127 (s), 1008 (m); HRMS (ESI-TOF) *m/z* $[M+H]^+$ calculated for $C_{13}H_{17}N_2O_3$: 249.1234. Found: 249.1230.

1-(Benzyl)-3-(3,4,5-trimethoxyphenyl)-pyrazole (34a, major) and 1-(benzyl)-4-(3,4,5-trimethoxyphenyl)-pyrazole (34b, minor). *N*-Benzylsydnone (200 mg, 1.14 mmol) and 3,4,5-trimethoxyphenylacetylene (436 mg, 2.27 mmol) were subjected to general procedure B, affording an inseparable mixture of pyrazoles **34a** and **34b** as an orange oil (239 mg, 64%, 9:1). ^{1}H NMR (400 MHz, $CDCl_3$) δ 3.87 (3H, s), 3.93 (6H, s), 5.36 (2H, s), 6.53 (1H, d, J = 2.5 Hz), 7.05 (2H, s), 7.21-7.28 (2H, m), 7.29-7.40 (4H, m); ^{13}C NMR (101 MHz, $CDCl_3$) δ 56.2, 56.3, 61.2, 103.0, 103.4, 106.5, 127.8, 128.1, 128.9, 129.5, 130.8, 136.7, 151.6, 153.6; FTIR: ν_{max} 2934 (w), 1587 (m), 1500 (m), 1423 (m), 1228 (s), 1125 (s), 1000 (s); HRMS (ESI-TOF) *m/z* $[M+H]^+$ calculated for $C_{19}H_{21}N_2O_3$: 325.1547. Found: 325.1550.

1-(Methyl)-3-([3-*tert*-butyldimethyloxy]-4-methoxyphenyl)-pyrazole (35a, major) and 1-(methyl)-4-([3-*tert*-butyldimethyloxy]-4-methoxyphenyl)-pyrazole (35b, minor). *N*-Methylsydnone (163 mg, 1.63 mmol) and (3-*tert*-butyldimethyloxy)-4-

methoxyphenylacetylene (787 mg, 3.00 mmol) were subjected to general procedure B, affording an inseparable mixture of pyrazole **35a** and **35b** was isolated as an orange oil (339 mg, 65%, 9:1). ^{1}H NMR (400 MHz, $CDCl_3$) δ 0.18 (6H, s), 1.01 (9H, s), 3.82 (3H, s), 3.93 (3H, s), 6.43 (1H, d, *J* = 2.5 Hz), 6.86 (1H, d, *J* = 8.5 Hz), 7.29 (1H, d, *J* = 2.0 Hz), 7.32-7.36 (2H, m); ^{13}C NMR (101 MHz, $CDCl_3$) δ -4.5, 18.6, 25.9, 39.1, 55.6, 102.5, 112.2, 118.6, 119.1, 126.9, 131.3, 145.2, 150.8, 151.6; FTIR: ν_{max} 2952 (w), 2930 (w), 2857 (w), 1508 (m), 1472 (m), 1271 (s), 1229 (s), 1135 (m), 992 (m), 915 (s); HRMS (ESI-TOF) *m/z* $[M+H]^+$ calculated for $C_{17}H_{27}N_2O_2Si$: 319.1836. Found: 319.1832.

1-(Benzyl)-3-([3-*tert*-butyldimethyloxy]-4-methoxyphenyl)-pyrazole (36a, major) and 1-(benzyl)-4-([3-*tert*-butyldimethyloxy]-4-methoxyphenyl)-pyrazole (36b, minor). *N*-Benzylsydnone (200 mg, 1.14 mmol) and (3-*tert*-butyldimethyloxy)-4-methoxyphenylacetylene (598 mg, 2.28 mmol) were subjected to general procedure B, affording an inseparable mixture of pyrazoles **36a** and **36b** as an orange oil (263 mg, 58%, >98:2). ^{1}H NMR (400 MHz, $CDCl_3$) δ 0.21 (6H, s), 1.05 (9H, s), 3.84 (3H, s), 5.35 (2H, s), 6.49 (1H, d, *J* = 2.5 Hz), 6.89 (1H, d, *J* = 8.5 Hz), 7.24-7.28 (2H, m), 7.31-7.38 (5H, m), 7.42 (1H, dd, *J* = 8.5, 2.0 Hz); ^{13}C NMR (101 MHz, $CDCl_3$) δ -4.5, 18.6, 25.9, 55.6, 56.1, 103.0, 112.2, 118.7, 119.2, 126.9, 127.8, 128.0, 128.8, 130.5, 136.8, 145.2, 150.8, 151.4; FTIR: ν_{max} 2952 (w), 2929 (w), 2857 (w), 1504 (m), 1472 (m), 1271 (s), 1229 (s), 1134 (m), 995 (m), 915 (m); HRMS (ESI-TOF) *m/z* $[M+H]^+$ calculated for $C_{23}H_{31}N_2O_2Si$: 395.2149. Found: 395.2147.

1-(Methyl)-3-(3,4,5-trimethoxyphenyl)-4-(3-hydroxy-4-methoxyphenyl)-pyrazole (37). Pyrazole **33** (543 mg, 2.19 mmol), NBS (389 mg, 2.19 mmol), 3-hydroxy-4-methoxyphenylboronic acid pinacol ester (822 mg, 3.29 mmol), XPhosPdG2 (172 mg, 0.219 mmol) and Na_2CO_3 (812 mg, 7.67 mmol) were subjected to general procedure F*i*, affording pyrazole **37** as a tan solid (551 mg, 68%). The product could be further purified by

recrystallization from pentane. M.p.: 46-48 °C; ^{1}H NMR (400 MHz, $CDCl_3$) δ 3.69 (6H, s), 3.72 (3H, s), 3.83 (3H, s), 3.95 (3H, s), 5.85 (1H, s), 6.74-6.77 (3H, m), 6.82 (1H, dd, *J* = 8.0, 2.0 Hz), 6.86 (1H, d, *J* = 8.0 Hz), 7.40 (1H, s); ^{13}C NMR (101 MHz, $CDCl_3$) δ 39.1, 55.9, 56.0, 61.0, 106.3, 111.9, 114.5, 120.8, 121.9, 125.4, 129.1, 130.2, 137.5, 144.7, 146.5, 148.3, 153.0; FTIR: ν_{max} 3405 (br), 2935 (w), 2831 (w), 1587 (m), 1556 (m), 1508 (m), 1462 (m), 1413 (s), 1234 (s), 1119 (s), 1002 (m); HRMS (ESI-TOF) *m/z* $[M+H]^+$ calculated for $C_{20}H_{23}N_2O_5$: 371.1601. Found: 371.1602; HPLC: Ret. Time: 12.82 min, Purity 95.2%.

1-(Benzyl)-3-(3,4,5-trimethoxyphenyl)-4-(3-hydroxy-4-methoxyphenyl)-pyrazole (38). Pyrazoles **34a** and **34b** (398 mg, 1.23 mmol, 9:1), NBS (218 mg, 1.23 mmol), 3-hydroxy-4-methoxyphenylboronic acid pinacol ester (461 mg, 1.85 mmol), XPhosPdG2 (97 mg, 0.123 mmol) and Na_2CO_3 (456 mg, 4.31 mmol) were subjected to general procedure F*i*, affording pyrazole **38** as a colourless solid (323 mg, 59%). The product could be further purified by recrystallization from ethyl acetate/40-60 petroleum ether. M.p.: 168-169 °C; ^{1}H NMR (400 MHz, $CDCl_3$) δ 3.72 (6H, s), 3.72 (3H, s), 3.84 (3H, s), 5.36 (2H, s), 5.64 (1H, s), 6.74 (1H, d, *J* = 2.0 Hz), 6.79 (2H, s), 6.82 (1H, dd, *J* = 8.0, 2.0 Hz), 6.86 (1H, d, *J* = 8.0 Hz), 7.31-7.42 (5H, m), 7.38 (1H, s); ^{13}C NMR (101 MHz, $CDCl_3$) δ 56.0, 56.1, 56.3, 61.0, 105.5, 111.8, 114.5, 121.2, 122.0, 125.4, 128.1, 128.3, 129.0, 129.2 (x2 C), 136.4, 137.6, 144.7, 146.4, 148.3, 153.1; FTIR: ν_{max} 2957 (w), 2933 (w), 1588 (m), 1558 (m), 1507 (m), 1418 (m), 1265 (m), 1240 (m), 1116 (s), 1004 (m); HRMS (ESI-TOF) *m/z* $[M+H]^+$ calculated for $C_{26}H_{27}N_2O_5$: 447.1914. Found: 447.1913; HPLC: Ret. Time: 16.29 min, Purity 95.8%.

1-(Methyl)-3-(3-hydroxy-4-methoxyphenyl)-4-(3,4,5-trimethoxyphenyl)-pyrazole (39). Pyrazoles **35a** and **35b** (125 mg, 0.392 mmol), NBS (70 mg, 0.392 mmol), potassium 3,4,5-trimethoxyphenyltrifluoroborate (159 mg, 0.580 mmol), XPhosPdG2 (31 mg, 0.039 mmol) and Na_2CO_3 (83 mg, 0.784 mmol) and K_2CO_3 (163 mg, 1.18 mmol) were to general procedure F*ii*, affording pyrazole **39** as a colourless solid (63 mg, 43%). The product could be

further purified by recrystallization from ethyl acetate/40-60 petroleum ether. M.p.: 171 °C; ^{1}H NMR (400 MHz, $CDCl_3$) δ 3.72 (6H, s), 3.86 (3H, s), 3.88 (3H, s), 3.95 (3H, s), 5.62 (1H, s), 6.50 (2H, s), 6.79 (1H, d, *J* = 8.5 Hz), 7.00 (1H, dd, *J* = 8.5, 2.0 Hz), 7.15 (1H, d, *J* = 2.0 Hz), 7.44 (1H, s); ^{13}C NMR (101 MHz, $CDCl_3$) δ 39.1, 56.1, 56.2, 61.1, 105.9, 110.5, 114.9, 120.6 (x2 C), 127.0, 129.0, 130.0, 136.9, 145.5, 146.4, 148.5, 153.2; FTIR: ν_{max} 3122 (br), 2965 (w), 2934 (w), 2838 (w), 1585 (m), 1462 (m), 1411 (s), 1338 (m), 1228 (s), 1127 (s), 1016 (m), 1000 (m); HRMS (ESI-TOF) *m/z* $[M+H]^+$ calculated for $C_{20}H_{23}N_2O_5$: 371.1601. Found: 371.1598; HPLC: Ret. Time: 13.49 min, Purity 95.3%.

1-(Benzyl)-3-(3-hydroxy-4-methoxyphenyl)-4-(3,4,5-trimethoxyphenyl)-pyrazole (40). Pyrazoles **36a** and **36b** (252 mg, 0.639 mmol), NBS (114 mg, 0.639 mmol), potassium 3,4,5-trimethoxyphenyltrifluoroborate (263 mg, 0.959 mmol), XPhosPdG2 (50 mg, 0.064 mmol) and Na_2CO_3 (135 mg, 1.28 mmol) and K_2CO_3 (265 mg, 1.92 mmol) were subjected to general procedure F*ii*, affording pyrazole **40** as a colourless solid (93 mg, 33%). The product could be further purified by recrystallization from ethyl acetate/40-60 petroleum ether. M.p.: 56-58 °C; ^{1}H NMR (400 MHz, $CDCl_3$) δ 3.71 (6H, s), 3.85 (3H, s), 3.89 (3H, s), 5.35 (2H, s), 5.54 (1H, s), 6.48 (2H, s), 6.80 (1H, d, *J* = 8.5 Hz), 7.02 (1H, dd, *J* = 8.5, 2.0 Hz), 7.19 (1H, d, *J* = 2.0 Hz), 7.30-7.40 (5H, m), 7.41 (1H, s); ^{13}C NMR (101 MHz, $CDCl_3$) δ 56.1, 56.2, 56.3, 61.1, 105.9, 110.5, 115.0, 120.7, 121.0, 128.1, 128.3, 129.0, 129.1, 136.5, 136.9, 145.5, 146.4, 148.5, 153.2 (two sp^2 carbons not observed); FTIR: ν_{max} 2935 (w), 1583 (m), 1455 (m), 1406 (m), 1234 (s), 1122 (s), 1001 (m); HRMS (ESI-TOF) *m/z* $[M+H]^+$ calculated for $C_{26}H_{27}N_2O_5$: 447.1914. Found: 447.1914; HPLC: Ret. Time: 16.34 min, Purity 97.0%.

Endothelial cell culture. Human Umbilical Vein Endothelial Cells (HUVECs) from pooled donors (Promocell, C-12203) were cultured on gelatin-coated dishes in endothelial cell basal medium (EBM) (Promocell: C-22010) supplemented with Endothelial Cell Growth Supplement Mix (Promocell: C-39215). The supplemented medium contained 2% foetal calf

serum (FCS), 0.4% Endothelial Cell Growth Supplement (ECGS), 0.1 ng/ml recombinant Human Epidermal Growth factor (hEGF), 1 ng/ml recombinant human Basic Fibroblast Growth Factor (hbFGF), 90 µg/ml heparin and 1 µg/ml hydrocortisone. Further low endotoxin heat inactivated FCS was then added to the medium to increase the final concentration to 10% (v/v). Cells were then kept at 37°C in a humidified incubator, were sub-cultured by trypsinisation when confluent and were used for up to 5 passages.

Immunofluorescence staining of the cell cytoskeleton. Immunofluorescence staining was used to visualize changes in cell morphology and the cytoskeleton. HUVECs were plated on 4 or 8 well fibronectin-coated Permanox chamber slides at 2.5 x 10^4 cells per well in 250 µl EBM for 8 well slides and 5 x 10^4 cells per well in 500 µl for 4 well slides.. Microtubules and actin filaments were stained according to general staining protocols described previously.[40]

For activity studies, various concentrations of each drug were prepared in EBM via systematic dilutions from a 20 mM stock in DMSO. The cells were treated with drug or vehicle control for 30 minutes. The media were then discarded and the cells fixed with 3.7% formalin in PBS for 10-20 minutes, and permeabilized in 0.1% triton X-100 prior to staining the cytoskeleton.

For recovery studies, cells were treated with drug or vehicle control for 30 or 60 minutes at 37 °C The medium was then removed and cells were washed four times with fresh medium containing serum. The cells were then placed in the incubator for 30 minutes; the washing procedure was then repeated and the cells incubated for a further 30 minutes.

Cell Proliferation Studies. The effects of various drugs on cell proliferation were established and GI_{50} values were obtained. 96-multiwell plates were coated with 0.2% gelatin in PBS for at least 30 minutes prior to culture. Cells were plated at 5 x 10^3/well in 100 µl medium and left to adhere for 24 hours. Different concentrations of drugs were then added

in 50 µl of EBM. A minimum of 8 wells were used for each drug concentration or vehicle control. The cells were incubated at 37 °C for 72 hours before the media were removed and cells were fixed with 3.7% formalin for 10-20 minutes. The wells were then washed four times with PBS and stained with 1% crystal violet (Sigma, Cat: C3886) solution in 10% ethanol for 10-20 minutes at room temperature. The plates were then repeatedly rinsed with water, dried overnight and then stained cells were lysed in 100 µl of 10% acetic acid. The absorbance at 590 nm was then recorded by a plate reader. The absorbance data was corrected against background (empty wells with lysis solution) and transformed into percentage growth inhibition for each drug concentration. Percentage growth inhibition values obtained from at least 3 independent experiments were plotted against the logarithm of drug concentration using GraphPad Prism software and GI_{50} values were established for each drug.

Endothelial Monolayer Permeability Assay. Cell culture inserts (Falcon: 353492) with a PET track etched membrane with pore size of 3 µm ($2.0 \pm 0.2 \times 10^5$ pores/cm^2) were coated (5 µg/mL) fibronectin for a minimum of 30 minutes. Cells were then plated at 5.0×10^4 cells per insert in 200 µl EBM. Each insert was placed in a well of a 24-multiwell companion plate, (Falcon: 353504) and 700 µL of EBM were added to the lower well. In each experiment 200 µl EBM without cells were added to one insert coated with fibronectin. The cells were kept at 37°C in a humidified incubator for 24 hours before the media were changed in both the wells and inserts. The cells were then kept at 37°C in a humidified incubator for a further 4 days. The cells were treated by the direct addition of 25 µL of drug solution into the insert and incubated at 37°C for 30 minutes. The media were removed from the inserts and replaced with 200 µL EBM containing FITC-dextran (0.8 mg/mL) (Sigma: 46945). Inserts

were then placed into the wells of a new 24-multiwell plate containing 700 μL of EBM and incubated at 37 °C in a humidified incubator for 30 minutes. Samples of media were taken from the lower well compartments and fluorescence was quantified on a plate reader at excitation 488, emission 525. The raw emission reading from each well was transformed into % emission relative to the well without cells, which was normalized to 100% emission (equivalent to 100% permeability). The perturbation of the monolayer was proportional to the emission of FITC-dextran that passed through the insert into the well.

Analysis of pMLC phosphorylation by Western Blotting. HUVECs were cultured in gelatin-coated 12-multiwell plates at at 5 x 10^4 cells per well in 1 mL EBM and kept at 37 °C in a humidified incubator for 7 days without media changes. Various concentrations of drugs were prepared in EBM *via* systematic dilutions from a 20 mM stock in DMSO except for Rho kinase inhibitor Y-27632 (Tocris), which was prepared as a 20 mM stock solution in dH_2O and used at a final concentration of 5 μM. Following drug exposure, cell culture media were discarded and proteins were extracted in 1 x NuPAGE LDS reducing sample buffer (LDS, ThermoFisher, Cat.: NP0008). The samples were then analyzed for MLC phosphorylation by western blotting using an antibody to dually phosphorylated MLC (Cell Signalling, #3674) as described previously.[40] Blots were stripped and reprobed using an antibody to actin (Sigma, Cat.:A4700).

***In Vivo* Analysis and Necrosis Scoring.** All animal care and experimental procedures were carried out in accordance with the UK Animals (Scientific Procedure) Act 1986, with local ethics committee approval and following published guidelines for the use of animals in cancer research.[44] Human colorectal adenocarcinoma SW1222 cells were injected s.c. (5 × 10^6 cells in 0.05 mL) into the rear dorsum of female severe combined immunodeficiency (SCID) mice (8–12 weeks old, 20–25 g). Three orthogonal diameters of subcutaneous tumors were measured using calipers and tumors were treated when they reached approximately 8

mm in mean diameter. Vehicle (50% Na_2CO_3/NaCl, 10 mL/kg), CA4P (100 mg/kg, 0.227 mmol/kg, in 50% Na_2CO_3/NaCl, 10 mL/kg) or a solution of **31** (81 mg/kg, 0.227 mmol/kg, 50% Na_2CO_3/NaCl, 10 mL/kg), was given as a single dose. Subcutaneous tumors were formalin-fixed, paraffin-embedded, and hematoxylin and eosin (H & E) stained 24 hours after treatment. The percentage of necrosis was measured from H&E sections and quantified according to a random points scoring (Chalkley) system.[42,43]

Statistics. Statistical analysis was carried out using GraphPad Prism 6 for Windows 8.1. The significance of differences between groups was assessed using a one-way ANOVA followed by a Tukey post-test, with $p<0.05$ considered significant.

Associated Content.

Supporting Information: ^1H, ^{13}C NMR spectra for selected compounds. This material is available free of charge via the Internet at http://pubs.acs.org.

Author Information.

Corresponding Authors:

* Email J.P.A.H.: j.harrity@sheffield.ac.uk. Phone: (0)114-22-29496.

* Email C.K.: c.kanthou@sheffield.ac.uk. Phone: (0)114 215 9052

*Email G. M. T.: g.tozer@sheffield.ac.uk. Phone: (0)114 215 9028

Author Contributions:

A.W.B. conducted all compound synthesis and *in vitro* evaluation. M.F. conducted *in vivo* work.

Notes:

The authors declare no competing financial interest.

Acknowledgements. The authors are grateful to Cancer Research UK and Yorkshire Cancer Research for financial support.

Abbreviations Used.

CA4, combretastatin A4; CA4P, disodium combretastatin A-4 3-*O*-phosphate, DAPI, 4',6-diamidino-2-phenylindole; FITC-dextran, fluorescein isothiocyanate-dextran; HUVEC, human umbilical vein endothelial cell; MLC, myosin light chain; MTD, maximum tolerated dose; PK/PD, pharmacokinetic/pharmacodynamics; pMLC, phosphorylated myosin light chain; ROCK, Rho-associated protein kinase; SCID, severe combined immunodeficiency; TBAF, tetrabutylammonium fluoride; TMS, trimethylsilyl; VDA, vascular disrupting agent; Y-27632, *trans*-4-[(1*R*)-1-aminoethyl]-*N*-4-pyridinylcyclohexanecarboxamide dihydrochloride.

References

[1] Folkman, J. What is the Evidence That Tumors Are Angiogenesis Dependent? *J. of the Natl. Cancer I.* **1990**, *82*, 4-7.

[2] Kanthou, C.; Tozer, G. M. Tumour Targeting by Microtubule-Depolymerising Vascular Disrupting Agents. *Expert Opin. Ther. Tar.* **2007**, *11*, 1443-1457.

[3] Baluk, P.; Hashizume, H.; McDonald, D. M. Cellular Abnormalities of Blood Vessels as Targets in Cancer. *Curr. Opin. Genet. Dev.* **2005**, *15*, 102-111.

[4] Tozer, G. M.; Kanthou, C.; Baguley, B. C. Disrupting Tumour Blood Vessels. *Nat. Rev. Cancer* **2005**, *5*, 423-435.

[5] Boyland, E.; Boyland, M. E. Studies in Tissue Metabolism: the Action of Colchicine and B Typhosus Extract. *Biochem. J.* **1937**, *31*, 454-460.

[6] Ludford, R. J. Factors Determining the Action of Colchicine on Tumour Growth. *Br. J. Cancer* **1948**, *2*, 75-86.

[7] Pettit, G. R.; Cragg, G. M.; Singh, S. B. Antineoplastic Agents, 122. Constituents of Combretum Caffrum. *J. Nat.Prod.* **1987**, *50*, 386-391.

[8] Lin, C. M.; Singh, S. B.; Chu, P. S.; Dempcy, R. O.; Schmidt, J. M.; Pettit, G. R.; Hamel, E. Interactions of Tubulin with Potent Natural and Synthetic Analogs of the Antimitotic Agent Combretastatin: a Structure-Activity Study. *Mol. Pharmacol.* **1988**, *34*, 200-208.

[9] Chaplin, D. J.; Pettit, G. R.; Parkins, C. S.; Hill, S. A. Antivascular Approaches to Solid Tumour Therapy: Evaluation of Tubulin Binding Agents. *Brit. J. Cancer. Suppl.* **1996**, *27*, S86-S88.

[10] Dark, G. G.; Hill, S. A.; Prise, V. E.; Tozer, G. M.; Pettit, G. R.; Chaplin, D. J. Combretastatin A-4, an Agent That Displays Potent and Selective Toxicity toward Tumor Vasculature. *Cancer Res.* **1997**, *57*, 1829-1834.

[11] Pettit, G. R.; Temple, C.; Narayanan, V. L.; Varma, R.; Simpson, M. J.; Boyd, M. R.; Rener, G. A.; Bansal, N. Antineoplastic Agents 322. Synthesis of Combretastatin A-4 Prodrugs. *Anticancer Drug Des.* **1995**, *10*, 299-309.

[12] McGown, A. T.; Fox, B. W. Structural and Biochemical Comparison of the Anti-Mitotic Agents Colchicine, Combretastatin A4 and Amphethinile. *Anticancer Drug Des.* **1989**, *3*, 249-254.

[13] Lin, C. M.; Ho, H. H.; Pettit, G. R.; Hamel, E. Antimitotic Natural Products Combretastatin A-4 and Combretastatin A-2: Studies on the Mechanism of Their Inhibition of the Binding of Colchicine to Tubulin. *Biochemistry* **1989**, *28*, 6984-6991.

[14] Monk, B. J.; Sill, M. W.; Walker, J. L.; Darus, C. J.; Sutton, G.; Tewari, K. S.; Martin, L. P.; Schilder, J. M.; Coleman, R. L.; Balkissoon, J.; Aghajanian, C. Randomized Phase II Evaluation of Bevacizumab Versus Bevacizumab Plus Fosbretabulin in Recurrent Ovarian, Tubal, or Peritoneal Carcinoma: An NRG Oncology/Gynecologic Oncology Group Study. *J. Clin. Oncol.* **2016**, *34*, 2279-2286.

[15] Cushman, M.; Nagarathnam, D.; Gopal, D.; Chakraborti, A. K.; Lin, C. M.; Hamel, E. Synthesis and Evaluation of Stilbene and Dihydrostilbene Derivatives as Potential Anticancer Agents That Inhibit Tubulin Polymerization. *J. Med. Chem.* **1991**, *34*, 2579-2588.

[16] Ohsumi, K.; Hatanaka, T.; Fujita, K.; Nakagawa, R.; Fukuda, Y.; Nihei, Y.; Suga, Y.; Morinaga, Y.; Akiyama, Y.; Tsuji, T. Syntheses and Antitumor Activity of Cis-Restricted Combretastatins: 5-Membered Heterocyclic Analogues. *Bioorg. Med. Chem. Lett.* **1998**, *8*, 3153-3158.

[17] Romagnoli, R.; Baraldi, P. G.; Brancale, A.; Ricci, A.; Hamel, E.; Bortolozzi, R.; Basso, G.; Viola, G. Convergent Synthesis and Biological Evaluation of 2-Amino-4-(3′,4′,5′-trimethoxyphenyl)-5-aryl Thiazoles as Microtubule Targeting Agents. *J. Med. Chem.* **2011**, *54*, 5144-5153.

[18] Romagnoli, R.; Baraldi, P. G.; Cruz-Lopez, O.; Lopez Cara, C.; Carrion, M. D.; Brancale, A.; Hamel, E.; Chen, L.; Bortolozzi, R.; Basso, G.; Viola, G. Synthesis and Antitumor Activity of 1,5-Disubstituted 1,2,4-Triazoles as Cis-Restricted Combretastatin Analogues. *J. Med.Chem.* **2010**, *53*, 4248-4258.

[19] Zhou, H.; Hallac, R. R.; Lopez, R.; Denney, R.; MacDonough, M. T.; Li, L.; Liu, L.; Graves, E. E.; Trawick, M. L.; Pinney, K. G.; Mason, R. P. Evaluation of Tumor Ischemia in Response to an Indole-Based Vascular Disrupting Agent Using BLI and (19)F MRI. *Am. J. Nucl. Med. Mol. Imaging* **2015**, *5*, 143-153.

[20] Zaninetti, R.; Cortese, S. V.; Aprile, S.; Massarotti, A.; Canonico, P. L.; Sorba, G.; Grosa, G.; Genazzani, A. A.; Pirali, T. A Concise Synthesis of Pyrazole Analogues of Combretastatin A1 as Potent Anti-Tubulin Agents. *ChemMedChem* **2013**, *8*, 633-643.

[21] Hadimani, M. B.; MacDonough, M. T.; Ghatak, A.; Strecker, T. E.; Lopez, R.; Sriram, M.; Nguyen, B. L.; Hall, J. J.; Kessler, R. J.; Shirali, A. R.; Liu, L.; Garner, C. M.; Pettit, G. R.; Hamel, E.; Chaplin, D. J.; Mason, R. P.; Trawick, M. L.; Pinney, K. G. Synthesis of a 2-Aryl-3-aroyl Indole Salt (OXi8007) Resembling Combretastatin A-4 with Application as a Vascular Disrupting Agent. *J. Nat. Prod.* **2013**, *76*, 1668-1678.

[22] Tron, G. C.; Pirali, T.; Sorba, G.; Pagliai, F.; Busacca, S.; Genazzani, A. A. Medicinal Chemistry of Combretastatin A4: Present and Future Directions. *J. Med. Chem.* **2006**, *49*, 3033-3044.

[23] Siebert, A.; Gensicka, M.; Cholewinski, G.; Dzierzbicka, K. Synthesis of Combretastatin A-4 Analogs and their Biological Activities. *Anticancer Agents Med. Chem.* **2016**, *16*, 942-960.

[24] Nguyen, T. L.; McGrath, C.; Hermone, A. R.; Burnett, J. C.; Zaharevitz, D. W.; Day, B. W.; Wipf, P.; Hamel, E.; Gussio, R. A Common Pharmacophore for a Diverse Set of Colchicine Site Inhibitors Using a Structure-Based Approach. *J. Med. Chem.* **2005**, *48*, 6107-6116.

[25] De Martino, G.; Edler, M. C.; La Regina, G.; Coluccia, A.; Barbera, M. C.; Barrow, D.; Nicholson, R. I.; Chiosis, G.; Brancale, A.; Hamel, E.; Artico, M.; Silvestri, R. New Arylthioindoles: Potent Inhibitors of Tubulin Polymerization. 2. Structure-Activity Relationships and Molecular Modeling Studies. *J. Med. Chem.* **2006**, *49*, 947-954.

[26] Sanghai, N.; Jain, V.; Preet, R.; Kandekar, S.; Das, S.; Trivedi, N.; Mohapatra, P.; Priyadarshani, G.; Kashyap, M.; Das, D.; Satapathy, S. R.; Siddharth, S.; Guchhait, S. K.;

Kundu, C. N.; Bharatam, P. V. Combretastatin A-4 inspired novel 2-aryl-3-arylamino-imidazo-pyridines/pyrazines as tubulin polymerization inhibitors, antimitotic and anticancer agents. *Med. Chem. Comm.* **2014**, *5*, 766-782.

[27] Xu, Q.; Qi, H.; Sun, M.; Zuo, D.; Jiang, X.; Wen, Z.; Wang, Z.; Wu, Y.; Zhang, W. Synthesis and Biological Evaluation of 3-Alkyl-1,5-Diaryl-1*H*-Pyrazoles as Rigid Analogues of Combretastatin A-4 with Potent Antiproliferative Activity. *PLoS ONE* **2015**, *10*, e0128710.

[28] Burja, B.; Čimbora-Zovko, T.; Tomić, S.; Jelušić, T.; Kočevar, M.; Polanc, S.; Osmak, M. Pyrazolone-Fused Combretastatins and Their Precursors: Synthesis, Cytotoxicity, Antitubulin Activity and Molecular Modeling Studies. *Bioorg. Med. Chem.* **2010**, *18*, 2375-2387.

[29] Singh, P.; Kaur, J.; Kaur, P.; Kaur, S. Search for MDR Modulators: Design, Syntheses and Evaluations of *N*-substituted Acridones for Interactions with *p*-glycoprotein and Mg^{2+}. *Bioorg. Med. Chem.* **2009**, *17*, 2423-2427.

[30] Lamberth, C. Pyrazole Chemistry in Crop Protection. *Heterocycles* **2007**, *71*, 1467-1502.

[31] Browne, D. L.; Harrity, J. P. A. Recent Developments in the Chemistry of Sydnones. *Tetrahedron* **2010**, *66*, 553-568.

[32] Decuypere, E.; Specklin, S.; Gabillet, S.; Audisio, D.; Liu, H.; Plougastel, L.; Kolodych, S.; Taran, F. Copper(I)-Catalyzed Cycloaddition of 4-Bromosydnones and Alkynes for the Regioselective Synthesis of 1,4,5-Trisubstituted Pyrazoles. *Org. Lett.* **2015,** *17*, 362-365.

[33] Kolodych, S.; Rasolofonjatovo, E.; Chaumontet, M.; Nevers, M.-C.; Créminon, C.; Taran, F. Discovery of Chemoselective and Biocompatible Reactions Using a High-Throughput Immunoassay Screening. *Angew. Chem. Int. Ed.* **2013**, *52*, 12056-12060.

[34] Specklin, S.; Decuypere, E.; Plougastel, L.; Aliani, S.; Taran, F. One-Pot Synthesis of 1,4-Disubstituted Pyrazoles from Arylglycines via Copper-Catalyzed Sydnone–Alkyne Cycloaddition Reaction. *J. Org. Chem.* **2014**, *79*, 7772-7777.

[35] Browne, D. L.; Helm, M. D.; Plant, A.; Harrity, J. P. A. A Sydnone Cycloaddition Route to Pyrazole Boronic Esters. *Angew. Chem. Int. Ed.* **2007**, *46*, 8656-8658.

[36] Browne, D. L.; Vivat, J. F.; Plant, A.; Gomez-Bengoa, E.; Harrity, J. P. A. Investigation of the Scope and Regiochemistry of Alkynylboronate Cycloadditions with Sydnones. *J. Am. Chem. Soc.* **2009,** *131*, 7762-7769.

[37] Comas-Barceló, J.; Foster, R. S.; Fiser, B.; Gomez-Bengoa, E.; Harrity, J. P. A. Cu-Promoted Sydnone Cycloadditions of Alkynes: Scope and Mechanism Studies. *Chem. Eur. J.* **2015**, *21*, 3257-3263.

[38] Brown, A. W.; Harrity, J. P. A. Direct Arylation of Sydnones with Aryl Chlorides toward Highly Substituted Pyrazoles. *J. Org. Chem.* **2015**, *80*, 2467-2472.

[39] Lunt, S.-J.; Akerman, S.; Hill, S. A.; Fisher, M.; Wright, V. J.; Reyes-Aldasoro, C. C.; Tozer, G. M.; Kanthou, C. Vascular Effects Dominate Solid Tumor Response to Treatment with Combretastatin A-4-phosphate. *Int. J. Cancer* **2011**, *129*, 1979-1989.

[40] Kanthou, C.; Tozer, G. M. The Tumor Vascular Targeting Agent Combretastatin A–4-Phosphate Induces Reorganization of the Actin Cytoskeleton and Early Membrane Blebbing in Human Endothelial Cells. *Blood* **2002**, *99*, 2060-2069.

[41] Strecker, T. E.; Odutola, S. O.; Lopez, R.; Cooper, M. S.; Tidmore, J. K.; Charlton-Sevcik, A. K.; Li, L.; Macdonough, M. T.; Hadimani, M. B.; Ghatak, A.; Liu, L.; Chaplin, D. J.; Mason, R. P.; Pinney, K. G.; Trawick, M. L. The vascular disrupting activity of OXi8006 in

endothelial cells and its phosphate prodrug OXi8007 in breast tumor xenografts. *Cancer Lett.* **2015**, *369*, 229-241.

[42] Chalkley, H. W. Method for the Quantitative Morphologic Analysis of Tissues. *J. Natl. Cancer I.* **1943**, *4*, 47-53.

[43] Williams, L. J.; Mukherjee, D.; Fisher, M.; Reyes-Aldasoro, C. C.; Akerman, S.; Kanthou, C.; Tozer, G. M., An *in vivo* Role for Rho Kinase Activation in the Tumour Vascular Disrupting Activity of Combretastatin A-4 3-O-phosphate. *Br. J. Pharmacol.* **2014**, 171, 4902-4913

[41] Workman, P.; Aboagye, E. O.; Balkwill, F.; Balmain, A.; Bruder, G.; Chaplin, D. J.; Double, J. A.; Everitt, J.; Farningham, D. A. H.; Glennie, M. J.; Kelland, L. R.; Robinson, V.; Stratford, I. J.; Tozer, G. M.; Watson, S.; Wedge, S. R.; Eccles, S. A. Guidelines for the Welfare and Use of Animals in Cancer Research. *Br. J. Cancer* **2010**, *102*, 1555-1577.

Table of Contents graphic

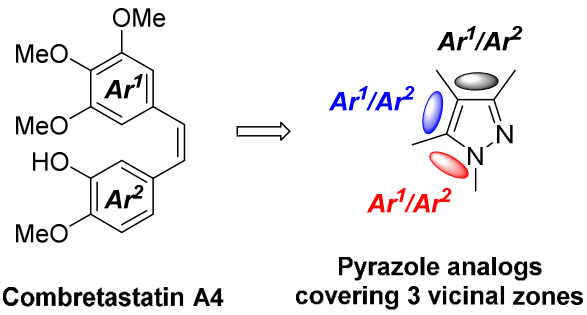

Combretastatin A4 **Pyrazole analogs covering 3 vicinal zones**

Table of Contents graphic

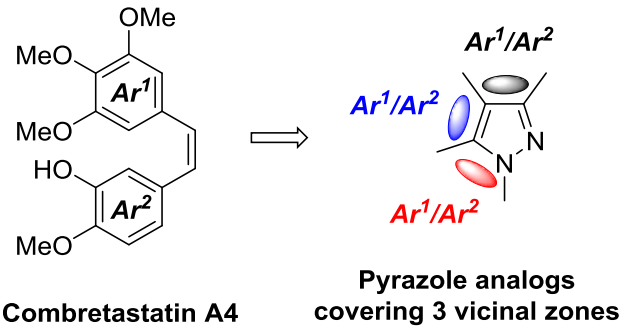

Combretastatin A4

Pyrazole analogs covering 3 vicinal zones